

Calculation of the continuum–lattice HQET matching for the complete basis of four–fermion operators: reanalysis of the B^0 – \bar{B}^0 mixing.

V. Giménez and J. Reyes¹

Dep. de Física Teórica and IFIC, Univ. de Valencia,
Dr. Moliner 50, E-46100, Burjassot, Valencia, Spain.

Abstract

In this work, we find the expressions of continuum HQET four-fermion operators in terms of lattice operators in perturbation theory. To do so, we calculate the one-loop continuum–lattice HQET matching for the complete basis of $\Delta B = 2$ and $\Delta B = 0$ operators (excluding penguin diagrams), extending and completing previous studies. We have also corrected some errors in previous evaluations of the matching for the operator O_{LL} . Our results are relevant to the lattice computation of the values of unknown hadronic matrix elements which enter in many very important theoretical predictions in B –meson phenomenology: B^0 – \bar{B}^0 mixing, τ_B and τ_{B_s} lifetimes, SUSY effects in $\Delta B = 2$ transitions and the B_s width difference $\Delta\Gamma_{B_s}$. We have reanalyzed our lattice data for the B_B parameter of the B^0 – \bar{B}^0 mixing on 600 lattices of size $24^3 \times 40$ at $\beta = 6.0$ computed with the SW-Clover and HQET lattice actions. We have used the correct lattice–continuum matching factors and boosted perturbation theory with tadpole improved heavy–light operators to reduce the systematic error in the evaluation of the renormalization constants. Our best estimate of the renormalization scale independent B –parameter is $\hat{B}_B = 1.29 \pm 0.08 \pm 0.06$, where the first error is statistical and the second is systematic coming from the uncertainty in the determination of the renormalization constants. Our result is in good agreement with previous results obtained by extrapolating Wilson data. As a byproduct, we also obtain the complete one-loop anomalous dimension matrix for four–fermion operators in the HQET.

PACS: 11.15.Ha, 12.38.Gc, 12.38.Bx, 12.39.Hg, 13.25.Hw, 14.40.Nd

¹Gobierno Vasco predoctoral Fellow

1 Introduction and Motivation.

B -hadron decays are a very important source of information on the physics of the standard model (SM) and beyond. In many important cases, long distance strong contributions to these processes can be separated into matrix elements of local operators. Lattice QCD can then be used to compute these non-perturbative parameters from first principles. A list of some four-fermion operators relevant to B -meson phenomenology is the following:

$\Delta B = 2$ operators

$$\begin{aligned} O_{LL(RR)} &= \bar{b} \gamma^\mu (1 \mp \gamma_5) q \bar{b} \gamma_\mu (1 \mp \gamma_5) q \\ O_{LL(RR)}^S &= \bar{b} (1 \mp \gamma_5) q \bar{b} (1 \mp \gamma_5) q \\ O_{LR(RL)} &= \bar{b} \gamma^\mu (1 \mp \gamma_5) q \bar{b} \gamma_\mu (1 \pm \gamma_5) q \\ O_{LR(RL)}^S &= \bar{b} (1 \mp \gamma_5) q \bar{b} (1 \pm \gamma_5) q \end{aligned} \quad (1)$$

$\Delta B = 0$ operators

$$\begin{aligned} Q_{LL(RR)} &= \bar{b} \gamma^\mu (1 \mp \gamma_5) q \bar{q} \gamma_\mu (1 \mp \gamma_5) b \\ Q_{LL(RR)}^S &= \bar{b} (1 \mp \gamma_5) q \bar{q} (1 \mp \gamma_5) b \\ Q_{LR(RL)} &= \bar{b} \gamma^\mu (1 \mp \gamma_5) q \bar{q} \gamma_\mu (1 \pm \gamma_5) b \\ Q_{LR(RL)}^S &= \bar{b} (1 \mp \gamma_5) q \bar{q} (1 \pm \gamma_5) b \end{aligned} \quad (2)$$

where q denotes a light quark u , d or s . The corresponding operators with a t^a (the generator of the SU(3) group) insertion, denoted by $Ot_{LL} \dots$ etc, will also be considered.

As is well known, O_{LL} determines the theoretical prediction of the B^0 - \bar{B}^0 mixing in the SM. Moreover, O_{LL} together with $O_{LL(RR)}^S$, O_{RR} and O_{LR}^S , parameterize SUSY effects in $\Delta B = 2$ transitions [1]. O_{LL} and O_{LL}^S determine the B_s width difference $\Delta\Gamma_{B_s}$ [2]. The $\Delta B = 0$ operators Q_{LL} and Q_{LR}^S , parameterize spectator effects in the τ_B and τ_{B_s} lifetimes [3]. For the four-fermion operators with a t^a insertion: $Ot_{LL}^S(RR)$ and Ot_{LR}^S contribute to SUSY effects in $\Delta B = 2$ transitions [1], and Qt_{LL} and Qt_{LR}^S to spectator effects in the B-meson lifetimes [3].

Our aim is to non-perturbatively evaluate the matrix elements between B -meson states of all the operators in eqs.(1) and (2), using lattice simulations of the b -quark in the HQET. These non perturbative parameters can also be measured in principle with propagating b quarks by simulating in the charm mass region and extrapolating to the b quark mass. The procedure to perform the transition from QCD to lattice HQET, a combination of analytic and numerical calculations, can be split into the following four steps:

First Step: *the continuum QCD – HQET matching.*

The QCD operators are expressed as linear combinations of HQET ones in the continuum at a given high scale, say, $\mu = m_b$.

Second Step: *running down to $\mu = a^{-1}$ in the HQET.*

The HQET operators obtained in step 1 at the high scale $\mu = m_b$ are evolved down to a lower scale $\mu = a^{-1}$, appropriate for lattice simulations, using the HQET NLO renormalization group equations.

Third Step: *continuum–lattice HQET matching.*

Having obtained the continuum HQET operators at the scale $\mu = a^{-1}$, they are expressed as a linear combination of lattice HQET operators at this scale. The procedure is very similar to step 1: two amplitudes are matched at one-loop order, one in the continuum HQET and the other in the lattice HQET.

Fourth Step: *lattice computation of the matrix elements.*

The matrix elements of the lattice HQET operators in Step 3, are measured by Monte Carlo numerical simulations on the lattice. Using these values and the chain of matching equations in steps 1 to 3, the matrix elements of the continuum QCD operators relevant to phenomenology can be determined.

In this work, we deal with step 3, i.e. we find the expressions of the continuum HQET operators in terms of lattice HQET ones using continuum and lattice perturbation theory at one loop. The calculation of steps 1 and 2, and the numerical simulation in step 4 are in progress and will be published elsewhere.

We would like to stress that a non perturbative determination of the lattice renormalization constants would be preferable because at the values of the coupling at which the simulations are performed, the one-loop perturbative corrections are not small, due to the appearance of tadpole diagrams. In principle, the Martinelli's *et al* [4] method for non perturbative renormalization may be utilized to avoid the problems with perturbation theory. Unfortunately, however, the application of the former to the HQET is not straightforward [5]. The key observation here is that HQET lattice simulations suggest that the finite heavy quark propagator in the Landau gauge has the form [6]

$$S(\vec{x}, t) = \delta(\vec{x}) \theta(t) A(t) e^{-(\lambda - \delta\bar{m})t} \quad (3)$$

where $A(t)$ is a smooth unknown function of t , λ is a constant and $\delta\bar{m}$ is the residual mass (also called the HQET mass counter-term). The latter is needed to remove the linear divergence in λ . On the one hand, the difference $m_S \equiv \lambda - \delta\bar{m}$ should be small in order to reduce $O(m_S a)$ terms. On the other hand, however, a too small m_S implies that the heavy quark propagator goes to a constant. This fact makes its numerical Fourier transform, a necessary ingredient in the Martinelli's *et al* method, very problematic due to the appearance of huge finite time effects of $O(e^{-m_S T})$, where T is the lattice time length. Therefore, the non perturbative calculation of renormalization constants in the HQET is difficult and requires more careful studies.

The paper is organized as follows. We begin by introducing the lagrangian of the HQET in the continuum and its discretized version which we will use in lattice simulations. The corresponding Feynman rules are derived for both heavy quarks and antiquarks. In section 3, we give the lattice lagrangian for light quarks and the

corresponding Feynman rules. The strategy of the calculation is presented in section 4. In this section, our renormalization prescription is discussed in detail. Moreover, we study the subtle point of the presence of evanescent operators and their effect on the matching and higher-order calculations. Then, we present the calculation details of the Feynman diagrams in the continuum and on the lattice HQET using several renormalization schemes. In section 6, our results for the one-loop continuum-lattice matching are given and compared with previous partial calculations. We also discuss the effects of a change of the continuum renormalization scheme. Then we reanalyze the B^0 - \bar{B}^0 mixing using the correct matching factors. Finally, we present our conclusions in section 8. In addition, we include one appendix where the relevant formula used in our calculation are collected.

2 Feynman rules for the continuum and discretized HQET lagrangians.

The Minkowski continuum lagrangian for a field $h(x)$ which annihilates a static heavy quark and for a field $\tilde{h}(x)$ which annihilates a static heavy antiquark is

$$\mathcal{L}_{HQET}^{cont}(x) = h^\dagger(x) i D_0 h(x) + \tilde{h}(x) i D_0 \tilde{h}^\dagger(x) \quad (4)$$

where $i D_\mu$ is the covariant derivative $i \partial_\mu + g t^a A_\mu^a(x)$ with $A_\mu^a(x)$ the gluon field and $t^a = \lambda^a/2$ the generators of the SU(3) color group normalized by $\text{tr}(t^a t^b) = \delta^{ab}/2$. A very important property of the HQET fields h and \tilde{h} is the fact that $\gamma_0 h = h$ and $\tilde{h} \gamma_0 = -\tilde{h}$. We will make extensive use of these properties in our calculation.

On the lattice, in Euclidean space, we have first to choose a discretization for the continuum covariant derivative D_μ , which has the correct continuum limit. Obviously there are many equivalent possibilities. The point is that the discretization we use in the perturbative calculation of the lattice operators must be the same as the one with which we perform the numerical simulation. Otherwise, the mismatch will generate spurious uncontrolled finite contributions to the final results. Our convention is to discretize backward in time, as first proposed by Eichten [7], so that the lattice HQET action is

$$\begin{aligned} S^{HQET} = & a^3 \sum_n \left\{ h^\dagger(n) \left[h(n) - U_4^\dagger(n - \hat{4}) h(n - \hat{4}) \right] \right. \\ & \left. + \tilde{h}(n) \left[U_4(n) \tilde{h}^\dagger(n + \hat{4}) - \tilde{h}^\dagger(n) \right] \right\} \end{aligned} \quad (5)$$

where n denotes a lattice site, $\hat{4}$ is the unit vector in the Euclidean time direction and U is defined in eq.(6) below.

From eqs.(4) and (5), it is easy to find the Feynman rules which are collected in Table 1. Some remarks are in order here. To perform a weak-coupling expansion in terms of g of the lattice lagrangian, we have parameterized the link variables as

$$U_\mu^\dagger(x) = e^{-iag A_\mu^a(x) t^a} \quad (6)$$

Quark	Minkowski HQET	Lattice HQET
Propagator	$\frac{i}{p^0 + i\epsilon}$	$\frac{a}{1 + \epsilon - e^{-i p_4 a}}$
quark-gluon vertex	$+ i g t_{\beta\alpha}^a g^{\mu 0}$	$- i g t_{\beta\alpha}^a \delta_{\mu 4} e^{-i p'_4 a}$
seagull vertex	does not exist	$- 1/2 a g^2 \delta_{\mu 4} \delta_{\nu 4} \{ t^a, t^b \}_{\beta\alpha} e^{-i p'_4 a}$
Antiquark	Minkowski HQET	Lattice HQET
Propagator	$\frac{i}{p^0 + i\epsilon}$	$\frac{a}{1 + \epsilon - e^{-i p_4 a}}$
quark-gluon vertex	$- i g t_{\alpha\beta}^a g^{\mu 0}$	$+ i g t_{\alpha\beta}^a \delta_{\mu 4} e^{-i p'_4 a}$
seagull vertex	does not exist	$+ 1/2 a g^2 \delta_{\mu 4} \delta_{\nu 4} \{ t^a, t^b \}_{\alpha\beta} e^{-i p'_4 a}$

Table 1: Feynman rules for the continuum Minkowski HQET and the discretized Euclidean HQET. Our conventions are discussed in the text.

where $A_\mu^a(x)$ is the gluon field and a is the lattice spacing. In Table 1, the propagator corresponds to a quark (antiquark) of momentum p , and a color conservation is understood. The quark–gluon vertex corresponds to an incoming quark (antiquark) of color α and momentum p , outgoing quark (antiquark) of color β and momentum p' and incoming gluon of color index a and Lorentz index μ . The lattice seagull vertex, which will give rise to tadpole diagrams, is defined as the quark–gluon vertex except for an additional incoming gluon with color index b and Lorentz index ν .

3 The light–quark Wilson and Clover actions.

The operators in eqs.(1) and (2) contain both a heavy and a light quark. The dynamics of the former is governed by the HQET lagrangian described in section 2. In this section, we consider the dynamics of the light degrees of freedom.

In the continuum, we use the standard QCD lagrangian for light quarks, which Feynman rules can be found in many text books (see, for example, ref.[8]).

On the lattice, and in our numerical simulations, light quark propagation is described through the Wilson action [9]

$$\begin{aligned}
S^W = & S_G[U] + a^4 \sum_{n,\mu} \left\{ -\frac{1}{2a} [\bar{\psi}(n) (r - \gamma_\mu) U_\mu(n) \psi(n + \hat{\mu}) \right. \\
& \left. + \bar{\psi}(n + \hat{\mu}) (r + \gamma_\mu) U_\mu^\dagger(n) \psi(n)] \right\} + a^4 \sum_n \left[\bar{\psi}(n) (m_0 + \frac{4r}{a}) \psi(n) \right] \quad (7)
\end{aligned}$$

where $S_G[U]$ is the standard Wilson plaquette action [9], r is the Wilson parameter and m_0 is the bare light fermion mass.

An important source of systematic error in lattice simulations is the finiteness of the lattice spacing, a . It is well-known that hadronic matrix elements computed with the Wilson action differ from the corresponding continuum ones by terms of $O(a)$. Some methods have been devised to reduce the cut-off dependence of the lattice hadronic matrix elements involving Wilson fermions. In this paper, we will apply the method of improvement first proposed by B. Sheikholeslami and R. Wohlert (SW) long ago [10], which has been deeply studied in ref.[11]. The main idea of this technique is to use the freedom we have in the definition of the discretized quark action to eliminate all terms of $O(a)$ from the lattice matrix elements, by adding some irrelevant $O(a)$ terms to the action (7) and redefining the lattice fields ψ .

The first recipe is to perform all calculations with the so-called SW-Clover action, given by

$$S^I = S^W - a^4 \sum_{n,\mu,\nu} \left[i g \frac{ar}{4} \bar{\psi}(n) \sigma_{\mu\nu} P_{\mu\nu}(n) \psi(n) \right] \quad (8)$$

where $P_{\mu\nu}(n)$ is the discretized field strength tensor defined by

$$P_{\mu\nu} = \frac{1}{4a^2} \sum_{i=1}^4 \frac{1}{2ig} (U_i - U_i^\dagger) \quad (9)$$

and the sum is over the four plaquettes in the μ - ν plane, stemming from the point n and taken counterclockwise.

The second recipe is the rule for constructing improved operators: the quark fields in lattice operators must be rotated

$$\psi' = \left(1 - a \frac{r}{2} \left[z \vec{D} - (1-z) m_0 \right] \right) \psi \quad (10)$$

where \vec{D} is the symmetric lattice covariant derivative and z is an arbitrary real number.

It can be demonstrated that on-shell lattice matrix elements of improved operators computed with the SW-Clover action do not contain $O((g^2)^n a \log^n a)$ terms for any value of z . We will take $z = 1$ so that the rotated operator do not depend on m_0 . The reason for this choice is that in this case perturbative calculations are more accurate [11].

The same method can be applied to the Eichten's action for heavy quarks in eq.(5). In ref.[12], it is shown, however, that for $O(a)$ improvement of on-shell matrix elements, no modification of the static quark propagator is needed. Therefore, in order to eliminate $O(a)$ terms from on-shell matrix elements of heavy-light operators, we have to perform the calculation with the SW-Clover action and rotate the light quark fields only. For heavy quarks, the usual unimproved Eichten's action (5) can be used.

For practical reasons, instead of rotating the fields in the numerical simulation, a rotation of the light-quark propagator is done [13]. This technique is equivalent to a new definition of the lattice quark fields and automatically improves the operators. Since

Propagator	$\left[1/a \sum_{\mu} (i \gamma_{\mu} \sin(p_{\mu} a)) + \left(m_0 + 2 \frac{r}{a} \sum_{\mu} \sin^2((p_{\mu} a)/2)\right)\right]^{-1}$
Wilson quark-gluon vert.	$(-i g) \frac{\lambda_{\beta\alpha}^a}{2} \left[\gamma_{\rho} \cos((p+p')_{\rho} \frac{a}{2}) - i r \sin((p+p')_{\rho} \frac{a}{2}) \right] e^{-ip'_{\rho} \frac{a}{2}} e^{ip_{\rho} \frac{a}{2}}$
Impr. quark-gluon vert.	$-g \frac{\lambda_{\beta\alpha}^a}{2} \frac{r}{2} \left[\sum_{\nu} (\sigma_{\rho\nu} \sin((p-p')_{\nu} a)) \cos((p-p')_{\rho} \frac{a}{2}) \right] e^{-ip'_{\rho} \frac{a}{2}} e^{ip_{\rho} \frac{a}{2}}$
Impr. quark-quark vert.	$-\frac{r}{4} \delta_{\alpha\beta} \sum_{\mu} \gamma_{\mu} [e^{ip_{\mu} a} - e^{-ip_{\mu} a}]$
quark-gluon-quark vert.	$(-i g a) \frac{r}{4} \frac{\lambda_{\beta\alpha}^a}{2} \gamma_{\rho} [e^{\pm ip_{\rho} a} + e^{\mp ip_{\rho} a} e^{-iq_{\rho} a}]$

Table 2: Feynman rules for the lattice Wilson and SW–Clover actions for light quarks.

this method is much easier to be implemented on the computer than the improvement with rotated fields, we will apply it in this paper.

To be definite, let us consider a generic $\Delta B = 2$ effective operator with arbitrary Γ_1 and Γ_2 dirac matrices

$$\tilde{O}(n) = \left(h^{\dagger}(n) \Gamma_1 \psi(n) \right) \left(\tilde{h}(n) \Gamma_2 \psi(n) \right) \quad (11)$$

The improved operator \tilde{O}^I is obtained by rotating the light-quark fields according to eq.(10), keeping terms of order $O(a^2)$ for the second method of improvement [13],

$$\begin{aligned} \tilde{O}^I(n) &= \tilde{O}(n) - a \frac{r}{2} \left[\left(h^{\dagger}(n) \Gamma_1 \vec{\not{D}} \psi(n) \right) \left(\tilde{h}(n) \Gamma_2 \psi(n) \right) \right. \\ &\quad \left. + \left(h^{\dagger}(n) \Gamma_1 \psi(n) \right) \left(\tilde{h}(n) \Gamma_2 \vec{\not{D}} \psi(n) \right) \right] \\ &\quad + a^2 \left(\frac{r}{2} \right)^2 \left(h^{\dagger}(n) \Gamma_1 \vec{\not{D}} \psi(n) \right) \left(\tilde{h}(n) \Gamma_2 \vec{\not{D}} \psi(n) \right) \end{aligned} \quad (12)$$

Similarly, we can improve the $\Delta B = 0$ operators.

From eqs.(7), (8) and (12), we can obtain the Feynman rules which are given in Table 2. In this Table, the propagator corresponds to a quark of momentum p and bare mass m_0 , and color conservation is understood. Both the Wilson and the improved quark–gluon vertex, the latter coming from the SW term in action (8), correspond to an incoming quark of color α and momentum p , outgoing quark of color β and momentum p' and incoming gluon of color index a and Lorentz index ρ . The other two vertices in Table 2 come from the rotation of the four-quark operators in eq.(12). In the improved quark–quark vertex we have an incoming or outgoing light-quark of color α and momentum p . In the quark–gluon–quark vertex, we have in addition an incoming gluon with momentum q , color index a and Lorentz index ρ and the sign of the momentum p in the exponentials is $+$ for an incoming light quark and $-$ for an outgoing one. For the gluon, we use the standard Wilson action [9].

4 The strategy: the subtle point of the renormalization scheme dependence.

Our aim is to express the continuum HQET operators at the scale $\mu = a^{-1}$ as a linear combination of lattice HQET operators at this scale in such a way that all continuum matrix elements be equal to their corresponding lattice counterparts up to one-loop order in perturbation theory.

The procedure is well known. The relation between the continuum and lattice operators to one-loop can be written as

$$O_i^{con} = \sum_j [\delta_{ij} + \frac{g^2}{16\pi^2} Z_{ij}] O_j^{lat} \quad (13)$$

By sandwiching eq.(13) between appropriate, but arbitrary, initial and final states, one can obtain the renormalization constants Z . In fact, some amplitudes are evaluated up to one-loop in perturbation theory both in the continuum and the lattice theory. After renormalization one gets

$$\langle O_i^{con(lat)} \rangle = \sum_j [\delta_{ij} + \frac{g^2}{16\pi^2} c_{ij}^{con(lat)}] \langle O_j^{con(lat)} \rangle^{(0)} \quad (14)$$

where (0) denotes the bare matrix element. Thus, the constants Z are obtained by simply subtracting at the scale given, $Z_{ij} = c_{ij}^{con} - c_{ij}^{lat}$; this is the matching procedure.

Note that the amplitudes can be regularized and renormalized using, in general, different schemes in both theories. Some subtle points to be stressed are the following:

1. the matching must be calculated with the same action as for the numerical simulation because the matching coefficients depend on the action to be simulated.
2. due to the breaking of chiral symmetry induced by the Wilson term for light quarks, the original operators can mix with lattice operators with different chirality.
3. the matching constants Z 's depend on the renormalization procedure chosen to define the operators in the continuum. This dependence will cancel with the remaining scheme dependence of the running in step 2 of the Introduction. This subtle point will be studied in detail in a forthcoming paper.

Therefore, it is very important to clearly define the regularization and renormalization schemes we utilize in our calculation. Many prescriptions can be chosen to regularize the corresponding Feynman integrals: NDR (Naïve Dimensional Regularization), DRED (Dimensional Reduction), HV (the 't Hooft-Veltman scheme) ... etc. Different regularization schemes will give rise to different finite parts in the amplitudes and hence to different matching coefficients. Having selected the regularization procedure, we have to choose the renormalization scheme to eliminate ultraviolet divergences, for example MOM (momentum subtraction), \overline{MS} ... etc.

Apparently, the continuum operators are now completely defined. A more careful analysis demonstrates, however, that this is not the case. In fact, there is another prescription to be set, namely, how to deal with the evanescent operators which unavoidably are generated [14]. We will explicitly show that different treatments of the evanescent operators will give rise to different finite contributions to the amplitude even when we return to four dimensions. The mechanism is clear: evanescent operators are operators which vanish in four dimensions, in other words, they are operators of order $O(n - 4)$, with $n = 4 + 2\epsilon$. When an evanescent operator is produced in a divergent diagram, terms of the form $1/\epsilon \times \text{evanescent}$ arise. Therefore, $O(\epsilon^0)$ contributions are generated and their value depend on the prescription we use to subtract the evanescent operators.

To sum, it is not sufficient to specify the scheme we use to renormalize our Feynman diagrams, we have also to define the prescription to eliminate the evanescent operators [14]. This fact results in the existence of families of \overline{MS} schemes which members differ in the treatment applied to the evanescent operators: we can, for instance, simply subtract them together with the divergent pole or project the amplitudes onto some convenient, but arbitrary, operator basis using some well-defined projectors. Note that in the second case, the projectors can be chosen in many different ways, each of which will define a different member in the corresponding scheme family. Of course, we can use our favourite prescription. It is immaterial with which one we perform the calculation. At the end, when the continuum QCD operator will be constructed in terms of HQET lattice operators, all dependence on the intermediate renormalization scheme used to define continuum HQET operators will drop and the final result will depend on the definition of the QCD operators only. The key point here is to be consistent during the whole procedure so that no spurious scheme dependence creep into our calculation.

5 The calculation.

We compute the matrix elements of the $\Delta B = 2$ operators in eq.(1) between an initial $B^0(\bar{b}q)$ state and a $\bar{B}^0(\bar{q}b)$ final state. For the $\Delta B = 0$ operators in eq.(2) we calculate the matrix elements between an initial and a final $\bar{B}^0(\bar{q}b)$ state neglecting penguin diagrams [3]. We set the light-quark mass to zero and take our momentum configuration to be vanishing incoming and outgoing momenta of both light and heavy quarks. To eliminate the infrared divergences which appear at zero external momenta, we give the gluon a mass, λ . This procedure is justified at one loop order.

On the lattice, the Feynman diagrams to be evaluated are depicted in fig. 1. The box represents an insertion of the four-fermion operator. The cross vertex stands for the contribution coming from the rotated part of the improved operator (see the entries for the improved quark-quark and quark-gluon-quark vertices in Table 2). Note that each light quark-gluon vertices in all diagrams consists of the Wilson vertex plus the improved contribution coming from the Clover action (see entries for the Wilson and

Improved quark-gluon vertices in Table 2). Ultraviolet divergences are regulated by the lattice cut-off, a .

In practice, we project the lattice amplitudes onto the Dirac basis $\mathcal{B} = \{\gamma_{\mp}, \gamma_{\mp\pm}, \gamma_{\mp}^s, \gamma_{\mp\pm}^s, \sigma_{\mp}\}$, where γ_{\mp} denotes the Dirac structure $\gamma^{\mu}(1 \mp \gamma_5) \otimes \gamma_{\mu}(1 \mp \gamma_5)$, $\gamma_{\mp\pm}$ is $\gamma^{\mu}(1 \mp \gamma_5) \otimes \gamma_{\mu}(1 \pm \gamma_5)$, γ_{\mp}^s is $(1 \mp \gamma_5) \otimes (1 \mp \gamma_5)$, $\gamma_{\mp\pm}^s$ is $(1 \mp \gamma_5) \otimes (1 \pm \gamma_5)$ and finally σ_{\mp} is $\sigma^{\mu\nu}(1 \mp \gamma_5) \otimes \sigma_{\mu\nu}(1 \mp \gamma_5)$. Notice also that $\sigma_{\mp\pm}$ vanishes in four dimensions. The projectors are defined by (the sign is + in Euclidean space and - in Minkowski space)

$$\begin{aligned}
P_{\gamma_{\mp}}(\Gamma_1 \otimes \Gamma_2) &= Tr[\Gamma_1 \gamma^{\mu}(1 \pm \gamma_5) \Gamma_2 \gamma_{\mu}(1 \pm \gamma_5)] / (32n(2-n)) \\
P_{\gamma_{\mp\pm}}(\Gamma_1 \otimes \Gamma_2) &= Tr[\Gamma_1 (1 \mp \gamma_5) \Gamma_2 (1 \pm \gamma_5)] / (32n) \\
P_{\gamma_{\mp}^s}(\Gamma_1 \otimes \Gamma_2) &= Tr[\Gamma_1 (1 \mp \gamma_5) \Gamma_2 (1 \mp \gamma_5)] (-n^2 + 9n - 16) / (256(n-2)) \\
&\quad \pm Tr[\Gamma_1 \sigma^{\mu\nu}(1 \mp \gamma_5) \Gamma_2 \sigma_{\mu\nu}(1 \mp \gamma_5)] / (256(2-n)) \\
P_{\gamma_{\mp\pm}^s}(\Gamma_1 \otimes \Gamma_2) &= Tr[\Gamma_1 \gamma^{\mu}(1 \pm \gamma_5) \Gamma_2 \gamma_{\mu}(1 \mp \gamma_5)] / (32n) \\
P_{\sigma_{\mp}}(\Gamma_1 \otimes \Gamma_2) &= Tr[\Gamma_1 \sigma^{\mu\nu}(1 \mp \gamma_5) \Gamma_2 \sigma_{\mu\nu}(1 \mp \gamma_5)] / (256n(n-1)(2-n)) \\
&\quad \pm Tr[\Gamma_1 (1 \mp \gamma_5) \Gamma_2 (1 \mp \gamma_5)] / (256(2-n))
\end{aligned} \tag{15}$$

where $n = 4$ ($n = 4 + 2\epsilon$) for a four (n) dimensional gamma algebra and $\Gamma_{1,2}$ are arbitrary Dirac matrices. On the lattice, γ_{μ} are the Euclidean gamma matrices satisfying the anticommutation relation $\{\gamma_{\mu}, \gamma_{\nu}\} = 2\delta_{\mu\nu}$ in four dimensions and $\sigma_{\mu\nu} = 1/2[\gamma_{\mu}, \gamma_{\nu}]$. With our definition, all operators in the basis \mathcal{B} project back onto themselves.

Since HQET fields h satisfy $\gamma_0 u_h = u_h$ and $\gamma_0 v_h = -v_h$, where u_h and v_h are the spinors for a heavy quark and antiquark, we can reduce the number of independent lattice amplitudes through the following Euclidean-space relationships

$$\begin{aligned}
&[\bar{u}_h \sigma^{\mu\nu}(1 \mp \gamma_5) v_q \bar{v}_h \sigma_{\mu\nu}(1 \mp \gamma_5) u_q] = \\
&\quad -4([\bar{u}_h(1 \mp \gamma_5) v_q \bar{v}_h(1 \mp \gamma_5) u_q] + [\bar{u}_h \gamma^{\mu}(1 \mp \gamma_5) v_q \bar{v}_h \gamma_{\mu}(1 \mp \gamma_5) u_q]) \\
&[\bar{u}_h \sigma^{\mu\nu}(1 \mp \gamma_5) v_q \bar{v}_q \sigma_{\mu\nu}(1 \mp \gamma_5) u_h] = \\
&\quad +4([\bar{u}_h(1 \mp \gamma_5) v_q \bar{v}_q(1 \mp \gamma_5) u_h] - [\bar{u}_h \gamma^{\mu}(1 \mp \gamma_5) v_q \bar{v}_q \gamma_{\mu}(1 \pm \gamma_5) u_h])
\end{aligned} \tag{16}$$

where u_q and v_q are the light quark and antiquark spinors. The first relation can be used to reduce $\Delta B = 2$ amplitudes and the second for $\Delta B = 0$ ones.

Moreover, since Fierz transformations are well defined in four dimensions, we have for $\Delta B = 2$ operators

$$\begin{aligned}
\mathcal{F}[\gamma^{\mu}(1 \mp \gamma_5) \otimes \gamma_{\mu}(1 \mp \gamma_5)] &= -[\gamma^{\mu}(1 \mp \gamma_5) \otimes \gamma_{\mu}(1 \mp \gamma_5)] \\
\mathcal{F}[\gamma^{\mu}(1 \mp \gamma_5) \otimes \gamma_{\mu}(1 \pm \gamma_5)] &= 2[(1 \pm \gamma_5) \otimes (1 \mp \gamma_5)] \\
\mathcal{F}[(1 \mp \gamma_5) \otimes (1 \mp \gamma_5)] &= [(1 \mp \gamma_5) \otimes (1 \mp \gamma_5)] \\
&\quad + \frac{1}{2}[\gamma^{\mu}(1 \mp \gamma_5) \otimes \gamma_{\mu}(1 \mp \gamma_5)]
\end{aligned} \tag{17}$$

where \mathcal{F} denotes the Fierz transformation and we have omitted for simplicity the external spinors.

In the continuum, only diagrams D_1 to D_6 contribute to the amplitude, for neither improved nor tadpole vertices appear (see Table 1). Ultraviolet divergences will be regulated using dimensional regularization. Unlike the lattice case, evanescent operators do arise in the continuum so that we have to give a prescription to deal with them.

If the gamma algebra is in n dimensions, as in NDR, the relations in eq.(17) are not valid because Fierz transformations are not well defined. Moreover, since the "magic" formulae for reducing the product of three gamma matrices is correct only in four dimensions, eq.(16) holds up to evanescent operator contributions. For instance, the continuation of the first relation in eq.(16) to n dimensions can be defined by

$$[\sigma^{\mu\nu} (1 \mp \gamma_5) \otimes \sigma_{\mu\nu} (1 \mp \gamma_5)] = f(n) ([\gamma^\mu (1 \mp \gamma_5) \otimes \gamma_\mu (1 \mp \gamma_5)] + [(1 \mp \gamma_5) \otimes (1 \mp \gamma_5)]) + \sigma_f \quad (18)$$

where $f(n)$ depends on the choice of the evanescent operator σ_f . A naïve prescription is to impose that $f(n) = 4$ as in four dimensions (notice that there is a change of sign between Minkowski and Euclidean spaces). However, we can equally well take $f(n) = n$ by redefining σ_f . A very interesting choice is $f(n) = 4(1 + 1/6\epsilon)$. This prescription is useful because leads to results which are Fierz symmetric. Notice that all three prescriptions are valid and differ only in the definition of the evanescent operator σ_f .

If we use DRED, where the positions and momenta are continued to n dimensions whereas all other tensors, in particular the gamma algebra, are leaving in four dimensions [15], eqs.(16) and (17) hold but new independent operators arise [16]

$$\begin{aligned} \bar{\gamma}_\mp &\equiv [\gamma^\mu (1 \mp \gamma_5) \otimes \gamma^\nu (1 \mp \gamma_5)] g_{\mu\nu}^{(n)} \equiv \frac{n}{4} \gamma_\mp + \gamma_\mp^f \\ \bar{\gamma}_{\mp\pm} &\equiv [\gamma^\mu (1 \mp \gamma_5) \otimes \gamma^\nu (1 \pm \gamma_5)] g_{\mu\nu}^{(n)} \equiv \frac{n}{4} \gamma_{\mp\pm} + \gamma_{\mp\pm}^f \\ \bar{\sigma}_\mp &\equiv [\sigma^{\mu\nu} (1 \mp \gamma_5) \otimes \sigma^{\rho\tau} (1 \mp \gamma_5)] g_{\mu\rho}^{(4)} g_{\nu\tau}^{(n)} \equiv \frac{n}{4} \sigma_\pm + \sigma_\mp^f \end{aligned} \quad (19)$$

where $g_{\mu\nu}^{(4)}$ and $g_{\mu\nu}^{(n)}$ are the metric tensors in four and n dimensions respectively. The Dirac structures γ_\mp , $\gamma_{\mp\pm}$ and σ_\mp are defined similarly to those with a bar except for the fact that Lorentz indices are contracted in four dimensions only. We have also defined three evanescent operators γ_\mp^f , $\gamma_{\mp\pm}^f$ and σ_\mp^f which will prove to be useful in the calculation. Notice that the operator $\bar{\sigma}_{\pm\mp}$, with the same notation as in eq.(19), is an evanescent operator because $\sigma_{\pm\mp}$ vanishes in four dimensions.

In the scheme proposed by 't Hooft and Veltman (HV) [17], γ_5 anticommutes with the gamma matrices in four dimensions but commutes with those in $n - 4$ dimensions. In addition, the rule to consistently define the coupling to chiral fields in the Standard Model implies that Dirac matrices in the four-fermion operators must be in four dimensions.

In order to show the dependence of the matching on the prescription chosen to define the continuum operators, we will perform the calculation in several schemes, namely,

NDR_ξ: NDR- \overline{MS} , where we project onto the basis \mathcal{B} in n dimensions with eq.(15).

The HQET magic relation for $\Delta B = 2$ operators (18), used to reduce the number of independent amplitudes, is taken with $f(n) = 4(1 + \xi\epsilon)$, where ξ is an arbitrary real number. A similar prescription is used for $\Delta B = 0$ operators.

DRED I: DRED- \overline{MS} , where we subtract with the basis \mathcal{B} plus the evanescent operators $\{\gamma_{\mp} - \bar{\gamma}_{\mp}, \gamma_{\mp\pm} - \bar{\gamma}_{\mp\pm}, \sigma_{\mp} - \bar{\sigma}_{\mp}, \bar{\sigma}_{\mp\pm}\}$.

DRED II: DRED- \overline{MS} , where we subtract with the basis \mathcal{B} plus the evanescent operators $\{\gamma_{\mp}^f, \gamma_{\mp\pm}^f, \sigma_{\mp}^f, \bar{\sigma}_{\mp\pm}\}$.

HV: HV- \overline{MS} , where we project onto the basis \mathcal{B} in four dimensions with eq.(15).

Notice that DRED II is equivalent to eliminate the evanescent operators by simply projecting them out because $P_i(\gamma_f) = 0$ (γ_f being any of the evanescent operators in the basis) for all projectors P_i in four dimensions in eq.(15).

6 The Results.

The continuum HQET operators \tilde{O}_{LL} , \tilde{O}_{LR} , \tilde{O}_{LL}^S and \tilde{O}_{LR}^S can be written in terms of lattice operators as

$$\begin{aligned}\tilde{O}_{LL}(\mu) &= \left(1 + \frac{g_s^2}{16\pi^2} \left[-4 \ln\left(\frac{\lambda^2}{\mu^2}\right) + \frac{4 + 3z + 3z'''}{3}\right] \right. \\ &\quad + \frac{g_{lat}^2}{16\pi^2} \left[4 \ln(\lambda^2 a^2) + (D_{LL} + D_{LL}^I + D_{LL}^{II})\right] \left. \right) O_{LL}^{lat} \\ &\quad + \frac{g_{lat}^2}{16\pi^2} (D_{RR} + D_{RR}^I + D_{RR}^{II}) O_{RR}^{lat} \\ &\quad + \frac{g_{lat}^2}{16\pi^2} (D_N + D_N^I) O_N^{lat} \tag{20}\end{aligned}$$

$$\begin{aligned}\tilde{O}_{LR}(\mu) &= \left(1 + \frac{g_s^2}{16\pi^2} \left[-7/2 \ln\left(\frac{\lambda^2}{\mu^2}\right) + \frac{23 + 18z - z' + 14z'''}{12}\right] \right. \\ &\quad + \frac{g_{lat}^2}{16\pi^2} \left[7/2 \ln(\lambda^2 a^2) + (D_{LR} + D_{LR}^I + D_{LR}^{II})\right] \left. \right) O_{LR}^{lat} \\ &\quad + \left(\frac{g_s^2}{16\pi^2} \left[3 \ln\left(\frac{\lambda^2}{\mu^2}\right) + \frac{-1 + 2z - z' - 2z'''}{2}\right] \right. \\ &\quad + \frac{g_{lat}^2}{16\pi^2} \left[-3 \ln(\lambda^2 a^2) + (\bar{D}_{RL}^S + \bar{D}_{RL}^{SI} + \bar{D}_{RL}^{SII})\right] \left. \right) O_{RL}^{lat S} \\ &\quad + \frac{g_{lat}^2}{16\pi^2} (D_M + D_M^I) O_M^{lat} \tag{21}\end{aligned}$$

$$\tilde{O}_{LL}^S(\mu) = \left(1 + \frac{g_s^2}{16\pi^2} \left[-4/3 \ln\left(\frac{\lambda^2}{\mu^2}\right) + \frac{1 + 4z + z' + z'' + 3z'''}{3}\right] \right)$$

$$\begin{aligned}
& + \frac{g_{lat}^2}{16\pi^2} \left[4/3 \ln(\lambda^2 a^2) + (D_{LL}^S + D_{LL}^{SI} + D_{LL}^{SII}) \right] \Big) O_{LL}^{lat S} \\
& + \left(\frac{g_s^2}{16\pi^2} \left[2/3 \ln\left(\frac{\lambda^2}{\mu^2}\right) - \frac{3 + z' + z'' + 3z'''}{24} \right] \right. \\
& + \left. \frac{g_{lat}^2}{16\pi^2} \left[-2/3 \ln(\lambda^2 a^2) + (\bar{D}_{LL} + \bar{D}_{LL}^I + \bar{D}_{LL}^{II}) \right] \right) O_{LL}^{lat} \\
& + \frac{g_{lat}^2}{16\pi^2} (\bar{D}_{RR} + \bar{D}_{RR}^I + \bar{D}_{RR}^{II}) O_{RR}^{lat} \\
& + \frac{g_{lat}^2}{16\pi^2} (D_P + D_P^I) O_P^{lat} \tag{22}
\end{aligned}$$

$$\begin{aligned}
\tilde{O}_{LR}^S(\mu) & = \left(1 + \frac{g_s^2}{16\pi^2} \left[-7/2 \ln\left(\frac{\lambda^2}{\mu^2}\right) + \frac{22 + 19z + 15z'''}{12} \right] \right. \\
& + \left. \frac{g_{lat}^2}{16\pi^2} + \left[7/2 \ln(\lambda^2 a^2) + (D_{LR}^S + D_{LR}^{SI} + D_{LR}^{SII}) \right] \right) O_{LR}^{lat S} \\
& + \left(\frac{g_s^2}{16\pi^2} \left[3/4 \ln\left(\frac{\lambda^2}{\mu^2}\right) + \frac{-2 + 3z - z'''}{8} \right] \right. \\
& + \left. \frac{g_{lat}^2}{16\pi^2} \left[-3/4 \ln(\lambda^2 a^2) + (\bar{D}_{RL} + \bar{D}_{RL}^I + \bar{D}_{RL}^{II}) \right] \right) O_{RL}^{lat} \\
& + \frac{g_{lat}^2}{16\pi^2} (D_Q + D_Q^I) O_Q^{lat} \tag{23}
\end{aligned}$$

where the analytical expressions for the lattice constants, D , can be found in the appendix A. Their numerical values for the Wilson parameter $r = 1.0$ are given in Table 3. In obtaining these numbers, we have used a reduced value of the heavy-quark self-energy constant $e = 4.53$ (to be compared with the non reduced one $e = 24.48$) which is consistent with fitting the time dependence of the Monte Carlo data through Ae^{Bt} . Notice that we have explicitly separated the contributions coming from the Wilson action (denoted by $D_{LL} \dots$ etc), the Clover action with improved operators not including $O(a^2)$ terms (denoted by $D_{LL}^I \dots$ etc) and including $O(a^2)$ corrections (denoted by $D_{LL}^{II} \dots$ etc). The new lattice operators O_N , O_M , O_P and O_Q are defined by

$$\begin{aligned}
O_N^{lat} & = O_{LR}^{lat} + O_{RL}^{lat} + 2(O_{LR}^{lat S} + O_{RL}^{lat S}) \\
O_M^{lat} & = 3/2(O_{LL}^{lat} + O_{RR}^{lat}) + 4(O_{LL}^{lat S} + O_{RR}^{lat S}) \\
O_P^{lat} & = O_{LR}^{lat} + O_{RL}^{lat} + 6(O_{LR}^{lat S} + O_{RL}^{lat S}) \\
O_Q^{lat} & = O_{LL}^{lat} + O_{RR}^{lat} + 8(O_{LL}^{lat S} + O_{RR}^{lat S}) \tag{24}
\end{aligned}$$

As can be seen from eqs.(20) to (23), the lattice transcriptions of the continuum operators depend on the renormalization scheme used to define the latter, including the prescription to deal with the evanescent operators. In fact, z to z''' parameterize

Constant	Wilson	Impr. I	Impr. II	Constant	Wilson	Impr. I	Impr. II
D_{LL}	-41.24	16.30	0.20	D_{LL}^S	-30.87	16.50	0.04
D_{RR}	-1.60	-0.40	-1.23	\bar{D}_{LL}	2.59	0.05	-0.04
D_N	-14.44	0.62	0	\bar{D}_{RR}	0.40	0.10	0.31
				D_P	1.81	-0.08	0
D_{LR}	-37.83	13.33	-0.94	D_{LR}^S	-37.83	13.33	-0.94
\bar{D}_{RL}^S	9.80	1.10	-0.73	\bar{D}_{RL}	2.45	0.28	-0.18
D_M	-7.22	0.31	0	D_Q	1.81	-0.08	0

Table 3: Numerical values of the constants D for the Wilson parameter $r = 1.0$.

Scheme	z	z'	z''	z'''
NDR $_{\xi}$	1	0	ξ	0
DRED I	0	0	0	0
DRED II	0	1	0	0
HV	0	0	0	1

Table 4: Values of the scheme dependent parameters z 's.

the scheme dependence in the continuum and are defined in Table 4. A interesting particular value of ξ is $\xi = 1/3$ which corresponds to a NDR scheme which preserves Fierz symmetry, i.e. renormalization and Fierz transformations commute in the continuum scheme NDR $_{1/3}$ at one-loop order.

Notice that the results in eqs.(20) to (23) are expressed in terms of two coupling constants, namely, the continuum, g_s , and the lattice, g_{lat} , ones. At one loop, however, we can consistently identify these two coupling constants because the difference is $O(\alpha_s^2)$. In this case, the logarithms combine giving $\log(a^2 \mu^2)$ so that the infrared regulator λ disappears, as it should be. Several recipes for improving the convergence of the lattice perturbative series by choosing a convenient perturbative expansion parameter have been proposed [19]. The choice of the optimal coupling constant is discussed for the particular case of the operator O_{LL} in the next section.

The lattice counterpart of the operator \tilde{O}_{LL} is already known. It was determined by Flynn *et al* [21] for the Wilson action and by Borrelli and Pittori [12] for the SW-Clover action. We have extended the calculation to all the HQET operators in eq.(1). Our results for \tilde{O}_{LL} agree with ref.[21] but disagree with ref.[12] in the sign of the contribution proportional to O_{RR}^{latt} coming from the Feynman diagram D_6 in fig. 1. This error propagates to the constant D_{RR}^I which correct value is given in Table 3 (to be compared with the value quoted in ref.[12], $D_{RR}^I = -2.58$.)

The operators with a t^a insertion, denoted by $\tilde{O}t_i$, can be readily obtained from the

corresponding expressions in eqs.(20) to (23) by simply replacing the lattice operators \tilde{O}_i with the operators $\tilde{O}t_i$ and the operators O_N, O_M, O_P and O_Q , defined in eq.(24), with $O_{N'}, O_{M'}, O_{P'}$ and $O_{Q'}$ given by

$$\begin{aligned}
O_{N'}^{lat} &= -\frac{1}{2} (O_{LR}^{lat} + O_{RL}^{lat}) - (O_{LR}^{lat S} + O_{RL}^{lat S}) \\
O_{M'}^{lat} &= -3/2 (O_{LL}^{lat} + O_{RR}^{lat}) - 2 (O_{LL}^{lat S} + O_{RR}^{lat S}) \\
O_{P'}^{lat} &= O_{LR}^{lat} + O_{RL}^{lat} - 6 (O_{LR}^{lat S} + O_{RL}^{lat S}) \\
O_{Q'}^{lat} &= O_{LL}^{lat} + O_{RR}^{lat} - 4 (O_{LL}^{lat S} + O_{RR}^{lat S}).
\end{aligned} \tag{25}$$

For the continuum HQET $\Delta B = 0$ operators, the results we have obtained are the following

$$\begin{aligned}
\tilde{Q}_{LL}(\mu) &= \left(1 + \frac{g_s^2}{16\pi^2} \left[-4 \ln\left(\frac{\lambda^2}{\mu^2}\right) + \frac{6 + 4z + 4z'''}{3} \right] \right. \\
&+ \frac{g_{lat}^2}{16\pi^2} \left[4 \ln(\lambda^2 a^2) + (E_{LL} + E_{LL}^I) \right] \Bigg) Q_{LL}^{lat} \\
&+ \left(\frac{g_s^2}{16\pi^2} \left[3 \ln\left(\frac{\lambda^2}{\mu^2}\right) - \frac{1 + 4z + z'}{2} \right] \right. \\
&+ \frac{g_{lat}^2}{16\pi^2} \left[-3 \ln(\lambda^2 a^2) + (Et_{LL} + Et_{LL}^I + Et_{LL}^{II}) \right] \Bigg) Qt_{LL}^{lat} \\
&+ \frac{g_{lat}^2}{16\pi^2} [\bar{E}t_{RL}^S + \bar{E}t_{RL}^{SI} + \bar{E}t_{RL}^{SII}] Qt_{RL}^{lat S} \\
&+ \frac{g_{lat}^2}{16\pi^2} (E_R + E_R^I) Q_R^{lat} \\
&+ \frac{g_{lat}^2}{16\pi^2} (Et_R + Et_R^I) Qt_R^{lat}
\end{aligned} \tag{26}$$

$$\begin{aligned}
\tilde{Q}_{LR}(\mu) &= \left(1 + \frac{g_s^2}{16\pi^2} \left[-4 \ln\left(\frac{\lambda^2}{\mu^2}\right) + \frac{6 + 4z + 4z'''}{3} \right] \right. \\
&+ \frac{g_{lat}^2}{16\pi^2} \left[4 \ln(\lambda^2 a^2) + (E_{LR} + E_{LR}^I) \right] \Bigg) Q_{LR}^{lat} \\
&+ \left(\frac{g_s^2}{16\pi^2} [2 - 2z + 2z'''] + \frac{g_{lat}^2}{16\pi^2} [Et_{LR} + Et_{LR}^I + Et_{LR}^{II}] \right) Qt_{LR}^{lat} \\
&+ \frac{g_{lat}^2}{16\pi^2} [Et_{RL} + Et_{RL}^I + Et_{RL}^{II}] Qt_{RL}^{lat} \\
&+ \frac{g_{lat}^2}{16\pi^2} (E_S + E_S^I) Q_S^{lat} \\
&+ \frac{g_{lat}^2}{16\pi^2} (Et_S + Et_S^I) Qt_S^{lat}
\end{aligned} \tag{27}$$

$$\begin{aligned}
\tilde{Q}_{LL}^S(\mu) = & \left(1 + \frac{g_s^2}{16\pi^2} \left[-4 \ln\left(\frac{\lambda^2}{\mu^2}\right) + \frac{6 + 4z + 4z'''}{3} \right] \right. \\
& + \frac{g_{lat}^2}{16\pi^2} \left[4 \ln(\lambda^2 a^2) + (E_{LL}^S + E_{LL}^{SI}) \right] \Big) Q_{LL}^{lat S} \\
& + \left(\frac{g_s^2}{16\pi^2} \left[4 \ln\left(\frac{\lambda^2}{\mu^2}\right) + \frac{-5 + z' + z'' + z'''}{2} \right] \right. \\
& + \frac{g_{lat}^2}{16\pi^2} \left[-4 \ln(\lambda^2 a^2) + (Et_{LL}^S + Et_{LL}^{SI} + Et_{LL}^{SII}) \right] \Big) Q_{LL}^{lat S} \\
& + \left(\frac{g_s^2}{16\pi^2} \left[-\ln\left(\frac{\lambda^2}{\mu^2}\right) + \frac{3 - z' - z''}{2} \right] \right. \\
& + \frac{g_{lat}^2}{16\pi^2} \left[\ln(\lambda^2 a^2) + (\bar{E}t_{LR} + \bar{E}t_{LR}^I + \bar{E}t_{LR}^{II}) \right] \Big) Q_{LR}^{lat} \\
& + \frac{g_{lat}^2}{16\pi^2} [\bar{E}t_{RL} + \bar{E}t_{RL}^I + \bar{E}t_{RL}^{II}] Q_{RL}^{lat} \\
& + \frac{g_{lat}^2}{16\pi^2} (E_T + E_T^I) Q_T^{lat} \\
& + \frac{g_{lat}^2}{16\pi^2} (Et_T + Et_T^I) Q_T^{lat} \tag{28}
\end{aligned}$$

$$\begin{aligned}
\tilde{Q}_{LR}^S(\mu) = & \left(1 + \frac{g_s^2}{16\pi^2} \left[-4 \ln\left(\frac{\lambda^2}{\mu^2}\right) + \frac{6 + 4z + 4z'''}{3} \right] \right. \\
& + \frac{g_{lat}^2}{16\pi^2} \left[4 \ln(\lambda^2 a^2) + (E_{LR}^S + E_{LR}^{SI}) \right] \Big) Q_{LR}^{lat S} \\
& + \left(\frac{g_s^2}{16\pi^2} \left[3 \ln\left(\frac{\lambda^2}{\mu^2}\right) - \frac{2 + 3z - z'''}{2} \right] \right. \\
& + \frac{g_{lat}^2}{16\pi^2} \left[-3 \ln(\lambda^2 a^2) + (Et_{LR}^S + Et_{LR}^{SI} + Et_{LR}^{SII}) \right] \Big) Q_{LR}^{lat S} \\
& + \frac{g_{lat}^2}{16\pi^2} [Et_{RR} + Et_{RR}^I + Et_{RR}^{II}] Q_{RR}^{lat} \\
& + \frac{g_{lat}^2}{16\pi^2} (E_U + E_U^I) Q_U^{lat} \\
& + \frac{g_{lat}^2}{16\pi^2} (Et_U + Et_U^I) Q_U^{lat} \tag{29}
\end{aligned}$$

where the analytical expressions for the lattice constants E can be found in the appendix A. Their numerical values for the Wilson parameter $r = 1.0$ and a reduced heavy-quark self-energy, are given in Table 5. Notice that, as before, we have explicitly separated the contributions coming from the Wilson action (denoted by $E_{LL} \dots$ etc), the Clover action with improved operators not including $O(a^2)$ terms (de-

Constant	Wilson	Impr. I	Impr. II	Constant	Wilson	Impr. I	Impr. II
E_{LL}	-38.40	13.41	0	E_{LL}^S	-38.40	13.41	0
Et_{LL}	10.60	1.30	-0.11	Et_{LL}^S	11.29	4.62	0.05
$\bar{E}t_{RL}^S$	4.80	1.19	3.69	$\bar{E}t_{LR}$	-0.69	-3.32	-0.16
E_R	9.63	-0.41	0	$\bar{E}t_{RL}$	1.20	0.30	0.92
Et_R	7.22	-0.31	0	E_T	9.63	-0.41	0
				Et_T	7.22	-0.31	0
E_{LR}	-38.40	13.41	0	E_{LR}^S	-38.40	13.41	0
Et_{LR}	8.53	-8.67	-0.60	Et_{LR}^S	10.60	1.30	-0.11
Et_{RL}	4.80	1.19	3.69	Et_{RR}	1.20	0.30	0.92
E_S	9.63	-0.41	0	E_U	9.63	-0.41	0
Et_S	7.22	-0.31	0	Et_U	7.22	-0.31	0

Table 5: Numerical values of the constants E for the Wilson parameter $r = 1.0$.

noted by $E_{LL}^I \dots$ etc) and including $O(a^2)$ corrections (denoted by $E_{LL}^{II} \dots$ etc). The new lattice operators Q_R , Q_S , Q_T and Q_U are defined by

$$\begin{aligned}
Q_R^{lat} &= -Q_{LR}^{lat} - Q_{RL}^{lat} + 2(Q_{LL}^{lat S} + Q_{RR}^{lat S}) \\
Q_S^{lat} &= -Q_{LL}^{lat} - Q_{RR}^{lat} + 2(Q_{LR}^{lat S} + Q_{RL}^{lat S}) \\
Q_T^{lat} &= Q_{LR}^{lat S} + Q_{RL}^{lat S} \\
Q_U^{lat} &= Q_{LL}^{lat S} + Q_{RR}^{lat S}
\end{aligned} \tag{30}$$

The operators $Qt_{R,S,T,U}$, with a t^a insertion, are defined as those in eq.(30) simply replacing Q with Qt .

The expressions of the $\Delta B = 0$ continuum HQET operators with a t^a can be obtained from eqs.(26) to (29) through the following procedure. Let $\tilde{Q}t$ be a generic continuum \tilde{Q} -operator with a t^a insertion. In terms of lattice operators, it can be written as

$$\tilde{Q}t = \sum_i Ft_i Qt_i^{lat} + \sum_i F_i Q_i^{lat}$$

where Ft_i and F_i are related to the corresponding constants of \tilde{Q} as follows

$$\left. \begin{aligned} Ft_i &= E_i + 7/6 Et_i \\ F_i &= 2/9 Et_i \end{aligned} \right\} \text{ if } i \neq R, S, T, U$$

$$\left. \begin{aligned} Ft_i &= -1/2 Et_i \\ F_i &= 1/6 E_i \end{aligned} \right\} \text{ if } i = R, S, T, U \tag{31}$$

As a byproduct of our calculation, we have also obtained the anomalous dimension

matrix, $\hat{\gamma}$, at one loop, $\hat{\gamma}^{(0)}$, defined by

$$\hat{\gamma} = \left(\frac{g^2}{16\pi^2} \right) \hat{\gamma}^{(0)} + \left(\frac{g^2}{16\pi^2} \right)^2 \hat{\gamma}^{(1)} \dots \quad (32)$$

for both the $\Delta B = 2$ and $\Delta B = 0$ operators. In the continuum dimensional regularization $\hat{\gamma}^{(0)}$ is simply twice the residue of the $1/\epsilon$ pole and on the lattice it is twice the coefficient of the $\log(\lambda^2 a^2)$. Therefore, we get for the $\Delta B = 2$ operators,

$$\hat{\gamma}^{(0)} = \begin{bmatrix} -3(N - \frac{1}{N}) & 0 & 0 & 0 \\ (1 + \frac{1}{N}) & -3N + 4 + \frac{7}{N} & 0 & 0 \\ 0 & 0 & -3(N - \frac{2}{N}) & 6 \\ 0 & 0 & 3/2 & -3(N - \frac{2}{N}) \end{bmatrix} \quad (33)$$

in the basis $\{\tilde{O}_{LL}, \tilde{O}_{LL}^S, \tilde{O}_{LR}, \tilde{O}_{RL}^S\}$ and where N is the number of colors.

For the $\Delta B = 0$ operators, we obtain the submatrices

$$\hat{\gamma}^{(0)} = \begin{bmatrix} -3(N - \frac{1}{N}) & 6 & 0 & 0 \\ \frac{3}{2}(1 - \frac{1}{N^2}) & -\frac{3}{N} & 0 & 0 \\ 0 & 0 & -3(N - \frac{1}{N}) & 6 \\ 0 & 0 & \frac{3}{2}(1 - \frac{1}{N^2}) & -\frac{3}{N} \end{bmatrix} \quad (34)$$

in the basis $\{\tilde{Q}_{LL}, \tilde{Q}_{tLL}, \tilde{Q}_{LR}^S, \tilde{Q}_{tLR}^S\}$, and

$$\hat{\gamma}^{(0)} = \begin{bmatrix} -3(N - \frac{1}{N}) & 0 & 0 & 0 \\ 0 & -3(N - \frac{1}{N}) & 0 & 0 \\ 0 & -2 & -3(N - \frac{1}{N}) & 8 \\ -\frac{1}{2}(1 - \frac{1}{N^2}) & -(N - \frac{2}{N}) & 2(1 - \frac{1}{N^2}) & (N - \frac{5}{N}) \end{bmatrix} \quad (35)$$

in the basis $\{\tilde{Q}_{LR}, \tilde{Q}_{tLR}, \tilde{Q}_{LL}^S, \tilde{Q}_{tLL}^S\}$.

7 Reanalysis of the B^0 - \bar{B}^0 mixing

As we said in the previous section, the value of the lattice constant D_{RR}^I quoted in ref.[12], is incorrect. This constant enters the continuum–lattice matching of the QCD operator O_{LL} , which matrix element between B^0 and \bar{B}^0 states determines the theoretical prediction of the B^0 - \bar{B}^0 mixing through the so-called B–parameter B_B [22]. In this section, we re–calculate the relevant renormalization constants and give the correct value of the B–parameter.

The B-parameter B_B is the ratio of the matrix element of the operator O_{LL} to its vacuum insertion approximation

$$B_B(\mu) \equiv \frac{\langle \bar{B}^0 | O_{LL}(\mu) | B^0 \rangle}{\frac{8}{3} |\langle 0 | A_0 | B^0 \rangle|^2} \quad (36)$$

The continuum QCD–lattice HQET matching for the operator O_{LL} and the heavy–light axial current $A_\mu = \bar{b} \gamma_\mu \gamma_5 q$ can be written as

$$\begin{aligned} O_{LL} &= Z_{O_L} O_{LL}^{lat} + Z_{O_R} O_{RR}^{lat} + Z_{O_N} O_N^{lat} + Z_{O_S} O_{LL}^{lat} \\ A_\mu &= Z_A A_\mu^{lat} \end{aligned} \quad (37)$$

where the Z ’s are matching (renormalization) factors which explicit expressions up to one–loop order are obtained by combining the results of steps 1 and 2 in the Introduction (we refer the reader to ref.[22] and references therein, where all the relevant formula are collected ²) and eq.(20) which corresponds to step 3 in the Introduction. The values of the constants D ’s which enter eq.(20) are given in Table 3. Notice that in all previous Clover HQET computations of B_B , the incorrect value of the constant $D_R = D_{RR} + D_{RR}^I + D_{RR}^{II} = -5.4$ was used, to be compared to the correct one $D_R = -3.23$. The physical value of the B-parameter is then given by

$$B_B(\mu) = \sum_{i=LL,RR,N,S} Z_{O_i}(\mu) Z_A^{-2}(\mu) \frac{\langle \bar{B}^0 | O_i^{lat}(a) | B^0 \rangle}{\frac{8}{3} |\langle 0 | A_4^{lat}(a) | B^0 \rangle|^2} \equiv \sum_i B_{O_i} \quad (38)$$

The numerical determination of the relevant lattice matrix elements, step 4 in the Introduction, is also discussed in detail in ref.[22]. We will take the values quoted in ref.[22] as input for our reanalysis.

We now turn to the delicate point of the improvement of our lattice perturbation theory results. We start by discussing the choice of the expansion parameter. Many different, but equivalent at one–loop level, definitions of the lattice coupling constant can be used in the perturbative calculation of the lattice–continuum matching. At scales $a^{-1} \approx 2-4$ GeV of our numerical simulations, we expect small non–perturbative effects in the renormalization constants because of asymptotic freedom. However, tadpole diagrams, which appear in lattice perturbation theory, give rise to large corrections and then to large uncertainties in the matching procedure. In refs.[18, 19], some recipes, usually refer to as Boosted Perturbation Theory (BPT), for choosing an optimal lattice coupling constant which would absorb many of the unwanted gluonic tadpole contributions are suggested. The claim is that the perturbative estimate of the renormalization constants obtained from BPT at low orders, is closer to the non–perturbative result than its Standard Perturbation Theory (SPT) counterpart. Unfortunately, there are several different prescriptions which application is, in some cases, ambiguous. In this work, we will calculate the renormalization constants for the B-parameter with the following definitions of the coupling constant:

²In eq.(19) of ref.[22] there is a misprint: the correct value of $\hat{\gamma}_{22}^{(0)}$ is $\hat{\gamma}_{22}^{(0)} = -8/3$.

SPT: Standard Perturbation Theory, $\alpha_s^{SPT} = g^2/(4\pi) = 6/(4\pi\beta)$. It is well known that this coupling leads to poor convergent perturbative series due to tadpole effects [18, 19]. We will use this coupling only for the sake of comparison.

NBPT(\square): Naïve Boosted Perturbation Theory based on the plaquette; $\alpha_s^{NBPT(\square)} = \alpha_s^{SPT}/u_0^4$, where $u_0 = (1/3 \text{Tr}(U_\square))^{1/4}$, was first introduced by Parisi [18]. In our simulation at $\beta = 6.0$, $1/3 \text{Tr}(U_\square) = 0.5937$.

NBPT(κ_c): Naïve Boosted Perturbation Theory based on the the critical Wilson hopping parameter, κ_c ; $\alpha_s^{NBPT(\kappa_c)} = \alpha_s^{SPT}/u_0^4$, where $u_0 = (8\kappa_c)^{-1}$. In our simulation at $\beta = 6.0$, $\kappa_c = 0.14543$ [22].

BPT($\ln(\square)$): Non-perturbative Boosted Perturbation Theory based on the plaquette's logarithm, $\ln(\square)$. Following ref.[19], to obtain the coupling $\alpha_s^{BPT(\ln(\square))}(q^*)$

1. we solve for $\alpha_V(3.41/a)$ the expansion of the plaquette's logarithm

$$\ln\left(\frac{1}{3} \text{Tr}(U_\square)\right) = -\frac{4\pi}{3} \alpha_V(3.41/a) [1 - (1.19 + 0.025 n_f) \alpha_V(3.41/a)];$$

2. then we evolve $\alpha_V(3.41/a)$ down to the Lepage–Mackenzie's optimal scale q^* (see below) through the two-loop renormalization group equation with the number of flavours $n_f = 0$ because our simulation is performed in the quenched approximation.

Having defined the coupling, it remains to fix the scale at which it will be evaluated. Since α_s^{SPT} , $\alpha_s^{NBPT(\square)}$ and $\alpha_s^{NBPT(\kappa_c)}$ do not run, no scale setting is necessary in contrast to the Lepage–Mackenzie's $\alpha_s^{BPT(\ln(\square))}(q^*)$. Taking into account that q^* is only meant to be a typical scale of the process under consideration, we may guess the scale through some physical arguments or, when the two-loop contributions are known, choose q^* so that the one-loop coefficient of the perturbative expansion vanishes. However, Lepage and Mackenzie have suggested a prescription to set q^* which consists in calculating the expectation value of $\ln(q^2)$ in the one-loop perturbative lattice contribution (the integrand of the integral defining the coefficient in front of $g^2/16\pi^2$ in eqs.(20) to (23) and eqs.(26) to (29)). It is clear that for divergent (μ dependent) renormalization constants, q^* depends on μ . Hernandez and Hill [25], however, have estimated q^* for heavy-light two-fermion operators using the Lepage–Mackenzie's prescription without including the divergent terms proportional to $\ln(\mu^2 a^2)$. Thus q^* is independent of the renormalization scale μ . We will use this scheme to determine the optimal scale q^* for Z_A . Further, the Lepage–Mackenzie's prescription is non ambiguous only if the operator under consideration does not mix with others under renormalization. In fact, if there is mixing, one can either calculate all renormalization constants at the same scale q^* or determine a separate scale for each mixing coefficient [20]. Since, in our case, the operators are divergent and do mix under renormalization, we do not know how to implement the Lepage–Mackenzie's prescription. In view of these difficulties, we choose to determine q^* for the heavy-light axial current renormalization

constant, Z_A , following ref.[25], but for four-fermion operators we will vary q^* in the range $1 \leq aq^* \leq \pi$, studying the dependence of B_B on this scale. In this study, for simplicity, we will use the same scale q^* for all mixing coefficients. Moreover, we will use the results from the range of q^* to estimate a systematic error.

Following Lepage and Mackenzie, we now construct tadpole improved lattice operators by non-perturbatively redefining the hopping parameter κ , $\tilde{\kappa} = \kappa u_0$, where the mean-field parameter u_0 can be taken to be the plaquette or $1/8\kappa_c$. This redefinition leads to the rescaling of the standard normalization of lattice quark fields, $\sqrt{2\kappa}$, with $\sqrt{u_0}$, $\sqrt{2\kappa} \sqrt{u_0}$, which is expected to remove tadpole contributions in the fermionic sector [19]. Notice that tadpole contributions appear even when a good expansion parameter is used. To be consistent, the one-loop perturbative tadpole contributions must be subtracted from our perturbative expressions by multiplying by $1/\sqrt{u_0}$ expanded up to one-loop. Moreover, all links operators $U(x)$ that appear in our lattice composite operators, should be rescaled with u_0 , $U(x)/u_0$, for the same reason as above. This method, usually referred to as Tadpole Improvement (TD), is expected to reorganize the perturbation series in such a way that TD lattice operators have smaller discretization errors and the lattice-to-continuum renormalization factors are nearer to unity. For the Wilson action, TD has been studied in ref.[19]. Its HQET counterpart is described in refs.[24, 25] to which we refer the reader for details. An important point to note is that for HQET quarks TD leads to a final result which is equivalent to the reduction of the heavy-quark self-energy constant e , already performed in the previous section. Therefore, heavy quark fields are already tadpole improved in our case. Light quark fields, however, are not. As explained before, TD involves multiplying all light-quark fields by $\sqrt{u_0}/\sqrt{u_0^{(1)}}$ where $u_0^{(1)}$ is the one-loop perturbative estimate of the mean-field parameter u_0 . For example, consider a generic heavy-light four-quark operator \tilde{O} . Its expression in terms of lattice operators is

$$\tilde{O} = (u_0) \left[1 + \frac{g_s}{16\pi^2} (D_O - D_{u_0}) \right] O^{lat TD} + \sum_i Z_{O_i} O_i^{lat} \quad (39)$$

where, to one-loop order, $u_0^{(1)} = 1 + \frac{g_s}{16\pi^2} D_{u_0}$. For two-quark heavy-light operators, like the Axial current A_μ , (u_0) in eq.(39) should be replaced with $\sqrt{u_0}$ and D_{u_0} by $D_{u_0}/2$, because now \tilde{O} contains only one light field. We will implement TD for both two and four-quark heavy-light operators and for all choices of the coupling constant except for SPT.

As can be seen from eq.(39), the value of q^* for the tadpole improved Z_A depends on the choice of the mean-field parameter u_0 . We have used two definitions of u_0 , namely the plaquette and $1/8\kappa_c$. Following ref.[25], where the calculation for the Wilson action was performed, and taking into account the contribution from the Clover action, we readily obtain for $r = 1.0$, $q_{A_\mu}^*(\square) a = 2.29$ for $u_0^4 = 1/3Tr(U_\square)$ and $q_{A_\mu}^*(\kappa_c) a = 2.63$ for $u_0 = 1/8\kappa_c$, to be compared to the Wilson result $q_{A_\mu}^*(\kappa_c) a = 2.18$ [25].

Finally, we would like to discuss our estimation of the systematic error due to the truncation of the perturbative series. The matching factors Z 's are the products of the

renormalization factors calculated in steps 1 to 3 in the Introduction, which have been computed independently up to $O(\alpha_s)$. In fact, the QCD operator O_{LL} at the scale m_b can be written in terms of HQET operators as follows

$$\begin{aligned} O_{LL}(m_b) &= C_L(\mu) \tilde{O}_{LL}(\mu) + C_S(\mu) \tilde{O}_{LL}^S(\mu) \\ C_L(\mu) &= 1 + \frac{g^2}{16\pi^2} X_L(\mu) \\ C_S(\mu) &= \frac{g^2}{16\pi^2} X_S(\mu) \end{aligned} \quad (40)$$

where μ is the renormalization scale in the HQET and the functions $X_L(\mu)$ and $X_S(\mu)$ have been calculated at NLO in refs.[26] (see also [22, 23]). The HQET operators \tilde{O}_{LL} and \tilde{O}_{LL}^S can, in turn, be expressed in terms of lattice HQET operators using eqs.(20) and (22),

$$\begin{aligned} \tilde{O}_{LL}(\mu) &= \left(1 + \frac{g^2}{16\pi^2} Y_{LL}(a\mu)\right) O_{LL}^{lat}(a) + \frac{g^2}{16\pi^2} Y_{RR} O_{RR}^{lat}(a) \\ &+ \frac{g^2}{16\pi^2} Y_N O_N^{lat}(a) \\ \tilde{O}_{LL}^S(\mu) &= \left(1 + \frac{g^2}{16\pi^2} Y_{LL}^S(a\mu)\right) O_{LL}^{lat\,S}(a) + \frac{g^2}{16\pi^2} \bar{Y}_{LL}(a\mu) O_{LL}^{lat}(a) \\ &+ \frac{g^2}{16\pi^2} \bar{Y}_{RR} O_{RR}^{lat}(a) + \frac{g^2}{16\pi^2} \bar{Y}_P O_P^{lat}(a) \end{aligned} \quad (41)$$

Adding all together, we get the QCD–HQET lattice matching for O_{LL} ,

$$\begin{aligned} O_{LL}(m_b) &= \left[1 + \frac{g^2}{16\pi^2} (X_L + Y_{LL}) + \left(\frac{g^2}{16\pi^2}\right)^2 (X_L Y_{LL} + X_S \bar{Y}_{LL})\right] O_{LL}^{lat}(a) \\ &+ \left[\frac{g^2}{16\pi^2} Y_{RR} + \left(\frac{g^2}{16\pi^2}\right)^2 (X_L Y_{RR} + X_S \bar{Y}_{RR})\right] O_{RR}^{lat}(a) \\ &+ \left[\frac{g^2}{16\pi^2} Y_N + \left(\frac{g^2}{16\pi^2}\right)^2 X_L Y_N\right] O_N^{lat}(a) \\ &+ \left[\frac{g^2}{16\pi^2} X_S + \left(\frac{g^2}{16\pi^2}\right)^2 X_S Y_{LL}^S\right] O_{LL}^{lat\,S}(a) \\ &+ \left[\left(\frac{g^2}{16\pi^2}\right)^2 X_S Y_P\right] O_P^{lat}(a) \end{aligned} \quad (42)$$

with obvious notation. We can organize the renormalization constants in two ways: including $O(\alpha_s^2)$ contributions coming from the products of the factors expanded separately to $O(\alpha_s)$ (method M_1) or excluding $O(\alpha_s^2)$ terms in eq.(42) (method M_2). Notice

that the method M_1 , in contrast to method M_2 , leads to results which depend on the renormalization scheme used in the definition of the intermediate continuum HQET operators. Since the lattice perturbative corrections are large, different prescriptions may result in rather big discrepancies in the final value of $B_B(m_b)$. We will view these differences as an estimation of the systematic error on B_B due to unknown higher order contributions to the perturbative renormalization constants. In refs.[22, 23], the method M_1 excluded terms of $O(\alpha_s^2)$ coming from the operator \tilde{O}_{LL}^S , i.e. they take $Y_{LL}^S = \bar{Y}_{LL} = \bar{Y}_{RR} = Y_P = 0$ in eq.(42). This is inconsistent because there is no reason for excluding these contributions when estimating the systematic error. Numerically the difference is very small except for the contribution proportional to O_P^{lat} due to the large value of its matrix element between B-meson states. This has been measured on the lattice using the same sample of gauge configurations as for O_{LL} , O_{RR} , O_N and O_{LL}^S . We refer the reader to ref.[27] for details.

Now we give our final results. In Tables 6 and 7, we present the numerical values of the renormalization constants and the B-parameter $B_B(m_b)$ for different choices of the coupling constant, the Lepage-Mackenzie's scale q^* and different ways in which we can organize the perturbative series (methods M_1 and M_2) [22]. Our results have been obtained using $\alpha_s(\mu)$ at NLO, $m_b = 5$ GeV, $\Lambda_{QCD}^{n_f=4} = 200$ MeV and four active quark flavours, $n_f = 4$. As can be seen, Z_{O_P} reduces the value of B_B from method M_2 by an amount smaller than the statistical errors (3-4%) and resulting in a reduction of the discrepancy between methods M_1 and M_2 . Further, the inclusion of the correct D_R gives a value of Z_{O_R} which is roughly one-half of the one used in refs.[22, 23]. Its non-negligible effect on B_B is to increase its value by an amount slightly larger than the statistical errors (about 6 – 8 %). By comparing the results obtained without and with TD in options 2 to 5 of Tables 6 and 7 for NBPT couplings, it is clear that the Tadpole improvement of the operators significantly reduces the difference between methods M_1 and M_2 and hence the systematic error. In fact, when TD is implemented results from methods M_1 and M_2 are completely compatible within statistical errors. We have also implemented TD for $\alpha^{BPT(\ln(\square))}(q^*)$ with two definitions of the mean-field parameter u_0 : using the plaquette or the hopping parameter. Again we found that the two definitions give results which are in perfect agreement within statistical errors. Moreover, the values of B_B obtained with $\alpha^{BPT(\ln(\square))}(q^*)$ are almost independent of q^* in the range $2 \leq q^* \leq \pi$ and compatible within statistical errors with those calculated with $\alpha^{NBPT(\square)}$ and $\alpha^{NBPT(\kappa_c)}$ for both methods M_1 and M_2 . For this reason, we estimate our final value of the B-parameter for the coupling $\alpha^{BPT(\ln(\square))}$ from the results in the interval $2 \leq q^* \leq \pi$. Finally, we have made the exercise of removing TD for this coupling. The main consequences are the following:

1. the value of the B parameter significantly depends on q^* . For instance, from method M_1 , B_B varies from 0.74(5) at $q^*a = 2$ to 0.86(5) at $q^*a = \pi$.
2. the discrepancy between methods M_1 and M_2 is much larger than with TD. For instance, from method M_2 , $B_B = 0.65(5)$ at $q^*a = 2$ and $B_B = 0.80(5)$ at $q^*a = \pi$, to be compared to the values from method M_1 given above.

Options			Z_{O_L}	Z_{O_R}	Z_{O_N}	Z_{O_S}	Z_{O_P}	Z_A
α_s^{SPT} 0.0796	M_1		0.7935	-0.0196	-0.0812	-0.1130	-0.0013	0.9045
		M_2	0.7658	-0.0236	-0.1008	-0.1229	0.0000	0.8999
$\alpha_s^{NBPT(\square)}$ 0.1341	M_1		0.7022	-0.0330	-0.1367	-0.1063	-0.0023	0.8145
		M_2	0.6539	-0.0397	-0.1698	-0.1229	0.0000	0.8067
$\alpha_s^{NBPT(\kappa_c)}$ 0.1458	M_1		0.6824	-0.0359	-0.1487	-0.1048	-0.0025	0.7950
		M_2	0.6297	-0.0432	-0.1847	-0.1229	0.0000	0.7866
$\alpha_s^{NBPT(\square)} \text{ TD}$ 0.1341	M_1		0.7302	-0.0330	-0.1367	-0.1084	-0.0023	0.8312
		M_2	0.7163	-0.0397	-0.1698	-0.1229	0.0000	0.8264
$\alpha_s^{NBPT(\kappa_c)} \text{ TD}$ 0.1458	M_1		0.7446	-0.0359	-0.1487	-0.1111	-0.0025	0.8326
		M_2	0.7387	-0.0432	-0.1847	-0.1229	0.0000	0.8282
q^*a	$\alpha_s^{BPT(\ln(\square))}$							
1.000	0.2449	M_1	0.7092	-0.0603	-0.2497	-0.1148	-0.0041	0.7993
		M_2	0.6977	-0.0725	-0.3102	-0.1229	0.0000	0.7957
2.000	0.1812	M_1	0.7061	-0.0396	-0.1636	-0.1111	-0.0030	0.7993
		M_2	0.7099	-0.0480	-0.2054	-0.1184	0.0000	0.7957
2.290	0.1727	M_1	0.7026	-0.0370	-0.1528	-0.1104	-0.0028	0.7993
		M_2	0.7083	-0.0449	-0.1921	-0.1177	0.0000	0.7957
2.630	0.1648	M_1	0.6986	-0.0347	-0.1430	-0.1098	-0.0027	0.7993
		M_2	0.7060	-0.0421	-0.1800	-0.1170	0.0000	0.7957
3.000	0.1580	M_1	0.6944	-0.0327	-0.1347	-0.1093	-0.0025	0.7993
		M_2	0.7033	-0.0397	-0.1698	-0.1163	0.0000	0.7957
π	0.1557	M_1	0.6929	-0.0320	-0.1320	-0.1091	-0.0025	0.7993
		M_2	0.7023	-0.0389	-0.1664	-0.1161	0.0000	0.7957

Table 6: Renormalization constants for different choices of the lattice coupling constants, q^* and options, see the text. The value of Z_A for the coupling $\alpha_s^{BPT(\ln(\square))}$ has been calculated at $q_{A_\mu}^* = 2.63$. For this coupling, TD is computed using $u_0 = 1/8\kappa_c$.

3. the average value of B_B is smaller than the TD one.

From Table 7, our best estimates of $B_B(m_b)$ and the renormalization invariant B -parameter, \hat{B}_B , are

$$\begin{aligned}
B_B(m_b) &= 0.81 \pm 0.05 \pm 0.03 \pm 0.02 \\
\hat{B}_B(m_b) &= 1.29 \pm 0.08 \pm 0.05 \pm 0.03
\end{aligned} \tag{43}$$

where the first error is statistical, the second is an estimate of the uncertainty due to the choice of the coupling constant and the optimal scale q^* and the third takes into account the contribution of higher-order terms to the renormalization constants. We have computed $B_B(m_b)$ using the NLO formulae.

Options			B_{O_L}	B_{O_R}	B_{O_N}	B_{O_S}	B_{O_P}	B_{B_d}
α_s^{SPT} 0.0796		M_1	0.912(43)	-0.023(1)	-0.097(6)	0.083(4)	-0.013(0)	0.862(44)
		M_2	0.889(42)	-0.027(1)	-0.122(7)	0.091(4)	0.000(0)	0.831(43)
$\alpha_s^{NBPT(\square)}$ 0.1341		M_1	0.995(47)	-0.047(2)	-0.202(13)	0.096(5)	-0.027(0)	0.816(49)
		M_2	0.945(45)	-0.057(2)	-0.256(16)	0.113(6)	0.000(0)	0.745(48)
$\alpha_s^{NBPT(\kappa_c)}$ 0.1458		M_1	1.015(48)	-0.053(2)	-0.231(15)	0.099(5)	-0.030(0)	0.800(51)
		M_2	0.957(45)	-0.066(3)	-0.293(19)	0.119(6)	0.000(0)	0.718(50)
$\alpha_s^{NBPT(\square)}$ TD 0.1341		M_1	0.993(47)	-0.045(2)	-0.194(12)	0.094(5)	-0.026(0)	0.823(49)
		M_2	0.986(47)	-0.055(2)	-0.244(15)	0.108(5)	0.000(0)	0.796(50)
$\alpha_s^{NBPT(\kappa_c)}$ TD 0.1458		M_1	1.010(48)	-0.049(2)	-0.210(13)	0.096(5)	-0.028(0)	0.819(50)
		M_2	1.012(48)	-0.059(2)	-0.264(17)	0.107(5)	0.000(0)	0.797(51)
q^*a	$\alpha_s^{BPT(\ln(\square))}$							
1.0000	0.2449	M_1	1.043(49)	-0.089(4)	-0.383(25)	0.108(5)	-0.050(0)	0.629(56)
		M_2	1.036(49)	-0.108(5)	-0.480(31)	0.116(6)	0.000(0)	0.564(59)
2.0000	0.1812	M_1	1.039(49)	-0.058(2)	-0.251(16)	0.104(5)	-0.036(0)	0.798(52)
		M_2	1.054(50)	-0.071(3)	-0.318(20)	0.112(5)	0.000(0)	0.777(55)
2.2900	0.1727	M_1	1.034(49)	-0.054(2)	-0.234(15)	0.104(5)	-0.034(0)	0.814(52)
		M_2	1.052(50)	-0.067(3)	-0.297(19)	0.112(5)	0.000(0)	0.799(54)
2.6300	0.1648	M_1	1.028(49)	-0.051(2)	-0.219(14)	0.103(5)	-0.032(0)	0.828(51)
		M_2	1.048(50)	-0.062(2)	-0.279(18)	0.111(5)	0.000(0)	0.818(53)
3.0000	0.1580	M_1	1.022(48)	-0.048(2)	-0.207(13)	0.103(5)	-0.031(0)	0.839(51)
		M_2	1.044(50)	-0.059(2)	-0.263(17)	0.110(5)	0.000(0)	0.833(53)
π	0.1557	M_1	1.019(48)	-0.047(2)	-0.202(13)	0.102(5)	-0.030(0)	0.842(50)
		M_2	1.043(49)	-0.058(2)	-0.258(16)	0.110(5)	0.000(0)	0.837(53)

Table 7: Values of each operator contribution to the B -parameter, and the total result, for different choices of the lattice coupling constants, q^* and options, see the text.

We have repeated the same analysis with the lattice data for the B - \bar{B} mixing from the UKQCD Collaboration obtained using the SW-Clover and HQET lattice actions at $\beta = 6.2$ [28]. The conclusions presented above remain the same and the final results turn out to be in perfect agreement with ours in eq.(43),

$$\begin{aligned}
B_B(m_b) &= 0.79 \pm 0.04 \pm 0.03 \pm 0.02 \\
\hat{B}_B(m_b) &= 1.26 \pm 0.06 \pm 0.05 \pm 0.03
\end{aligned} \tag{44}$$

Note also that we do not see any dependence of our results on the lattice spacing a , within errors.

These numbers are to be compared with our previous result [22]: $\hat{B}_B(m_b) = 1.08 \pm 0.06 \pm 0.08$, obtained with the same lattice data but with the incorrect values of the renormalization constants and without tadpole improvement for the four-fermion

operators. Unlike our previous result, our best estimates in eq.(43) are now in good agreement with previous determinations of the B -parameter calculated by extrapolating Wilson data from the charm to the bottom mass (see Table 4 of ref.[22]).

8 Conclusions

In this paper we have determined the expressions of all $\Delta B = 2$ and $\Delta B = 0$ four-fermion HQET continuum operators in terms of HQET lattice ones using perturbation theory up to one loop. This calculation is a necessary ingredient in the procedure to measure the unknown values of some important matrix elements of QCD four-fermion operators by simulating them with lattice HQET. The calculation has been performed in four continuum renormalization schemes, NDR, DRED I, DRED II and HV, and for three lattice actions, Wilson, SW-Clover with rotated fermion fields and SW-Clover with rotated propagators.

We have also discussed the subtleties associated with the renormalization scheme dependence of our results. The effects of evanescent operators which appear in intermediate steps of the computation have been identified and clarified.

As a byproduct of our calculation, we have also obtained the one-loop anomalous dimension matrices for both the $\Delta B = 2$ and $\Delta B = 0$ HQET operators.

We have found and corrected an error in the one-loop result quoted in [12] for the lattice-continuum matching of the operator O_{LL} , which matrix element between B -meson states determines the value of the B_B parameter of the B - \bar{B} mixing. Then we have reanalyzed the lattice data measured in ref.[22] with the correct renormalization constant. We have used Boosted perturbation theory with tadpole improvement to reduce the systematic uncertainties in the renormalization constants due to the truncation of the perturbative series. Our value for the B_B parameter turns out to be larger and has a smaller systematic error than in previous studies with static heavy quarks. Further, it is compatible with the results obtained by extrapolating lattice Wilson data.

Acknowledgments

We thank G. Martinelli for very useful discussions. We also thank M. di Pierro and C. T. Sachrajda for helpful discussions. We acknowledge the partial support by CICYT under grant number AEN-96/1718. J.R. thanks the Departamento de Educacion of the Gobierno Vasco for a predoctoral fellowship.

Appendix A Analytical expressions of the constants.

In this appendix we give the analytical expressions for the lattice constants which enter the continuum–lattice matching relations.

$\Delta B = 2$ operators.

Operator O_{LL}

$$\begin{aligned}
D_{LL} &= -1/3 v - 10/3 d_1 - 1/3 c - 4/3 e - 4/3 f \\
D_{LL}^I &= -1/3 v^I + 8/3 (l + m) + 1/3 s - 4/3 f^I - 10/3 n \\
D_{LL}^{II} &= \delta_L \\
D_{RR} &= 4/3 w \\
D_{RR}^I &= 4/3 w^I - 2/3 (l + m) + 1/3 s \\
D_{RR}^{II} &= \delta_R \\
D_N &= 2 d_2 \\
D_N^I &= -4 d^I - 2 q + 2 h
\end{aligned} \tag{A.1}$$

Operator O_{LR}

$$\begin{aligned}
D_{LR} &= w + 1/6 J_1 - 7/3 d_1 + 1/6 c - 4/3 e - 4/3 f \\
D_{LR}^I &= w^I + 13/6 (l + m) + 1/4 s + 1/6 J_2 - 4/3 f^I - 7/3 n \\
D_{LR}^{II} &= 3/4 \delta_R + 1/6 J_3 \\
\bar{D}_{RL}^S &= 2/3 w + J_1 + 2 d_1 + c \\
\bar{D}_{RL}^{SI} &= 2/3 w^I - 1/3 (l + m) + 1/6 s + J_2 + 2 n \\
\bar{D}_{RL}^{SII} &= 1/2 \delta_R + J_3 \\
D_M &= d_2 \\
D_M^I &= -2 d^I - q + h
\end{aligned} \tag{A.2}$$

Operator O_{LL}^S

$$\begin{aligned}
D_{LL}^S &= -2/9 v + 8/9 J_1 - 4/3 d_1 + 2/3 c - 4/3 e - 4/3 f \\
D_{LL}^{SI} &= -2/9 v^I + 8/3 (l + m) + 2/9 s + 8/9 J_2 - 4/3 f^I - 4/3 n \\
D_{LL}^{SII} &= 2/3 \delta_L + 8/9 J_3 \\
\bar{D}_{LL} &= 1/36 v + 2/9 J_1 + 1/2 d_1 + 1/4 c \\
\bar{D}_{LL}^I &= 1/36 v^I - 1/36 s + 2/9 J_2 + 1/2 n
\end{aligned}$$

$$\begin{aligned}
\bar{D}_{LL}^{II} &= -1/12 \delta_L + 2/9 J_3 \\
\bar{D}_{RR} &= -1/3 w \\
\bar{D}_{RR}^I &= -1/3 w^I + 1/6 (l + m) - 1/12 s \\
\bar{D}_{RR}^{II} &= -1/4 \delta_R \\
D_P &= -1/4 d_2 \\
D_P^I &= 1/2 d^I + 1/4 q - 1/4 h
\end{aligned} \tag{A.3}$$

Operator O_{LR}^S

$$\begin{aligned}
D_{LR}^S &= w + 1/6 J_1 - 7/3 d_1 + 1/6 c - 4/3 e - 4/3 f \\
D_{LR}^{SI} &= w^I + 13/6 (l + m) + 1/4 s + 1/6 J_2 - 4/3 f^I - 7/3 n \\
D_{LR}^{SII} &= 3/4 \delta_R + 1/6 J_3 \\
\bar{D}_{RL} &= 1/6 w + 1/4 J_1 + 1/2 d_1 + 1/4 c \\
\bar{D}_{RL}^I &= 1/6 w^I - 1/12 (l + m) + 1/24 s + 1/4 J_2 + 1/2 n \\
\bar{D}_{RL}^{II} &= 1/8 \delta_R + 1/4 J_3 \\
D_Q &= -1/4 d_2 \\
D_Q^I &= 1/2 d^I + 1/4 q - 1/4 h
\end{aligned} \tag{A.4}$$

$\Delta B = 0$ operators.

Operator Q_{LL}

$$\begin{aligned}
E_{LL} &= -8/3 d_1 - 4/3 e - 4/3 f \\
E_{LL}^I &= 8/3 (l + m) - 8/3 n - 4/3 f^I \\
Et_{LL} &= J_1 + 2 d_1 + c \\
Et_{LL}^I &= J_2 + 2 n \\
Et_{LL}^{II} &= J_3 \\
\bar{E}t_{RL}^S &= -4 w \\
\bar{E}t_{RL}^{SI} &= -4 w^I + 2 (l + m) - s \\
\bar{E}t_{RL}^{SII} &= -3 \delta_R \\
E_R &= -4/3 d_2 \\
E_R^I &= 4/3 (2 d^I + q - h) \\
Et_R &= -d_2 \\
Et_R^I &= 2 d^I + q - h
\end{aligned} \tag{A.5}$$

Operator Q_{LR}

$$\begin{aligned}
E_{LR} &= -8/3 d_1 - 4/3 e - 4/3 f \\
E_{LR}^I &= 8/3 (l + m) - 8/3 n - 4/3 f^I \\
Et_{LR} &= v + 2 d_1 + c \\
Et_{LR}^I &= v^I - s + 2 n \\
Et_{LR}^{II} &= -3 \delta_L \\
Et_{RL} &= -4 w \\
Et_{RL}^I &= -4 w^I + 2 (l + m) - s \\
Et_{RL}^{II} &= -3 \delta_R \\
E_S &= -4/3 d_2 \\
E_S^I &= 4/3 (2 d^I + q - h) \\
Et_S &= -d_2 \\
Et_S^I &= 2 d^I + q - h
\end{aligned} \tag{A.6}$$

Operator Q_{LL}^S

$$\begin{aligned}
E_{LL}^S &= -8/3 d_1 - 4/3 e - 4/3 f \\
E_{LL}^{SI} &= 8/3 (l + m) - 4/3 f^I - 8/3 n \\
Et_{LL}^S &= 4/3 J_1 - 1/3 v + 2 d_1 + c \\
Et_{LL}^{SI} &= -1/3 v_I + 1/3 s + 4/3 J_2 + 2 n \\
Et_{LL}^{SII} &= \delta_L + 4/3 J_3 \\
\bar{E}t_{LR} &= -1/3 J_1 + 1/3 v \\
\bar{E}t_{LR}^I &= 1/3 v^I - 1/3 s - 1/3 J_2 \\
\bar{E}t_{LR}^{II} &= -\delta_L - 1/3 J_3 \\
\bar{E}t_{RL} &= -w \\
\bar{E}t_{RL}^I &= -w^I + 1/2 (l + m) - 1/4 s \\
\bar{E}t_{RL}^{II} &= -3/4 \delta_R \\
E_T &= -4/3 d_2 \\
E_T^I &= 4/3 (2 d^I + q - h) \\
Et_T &= -d_2 \\
Et_T^I &= 2 d^I + q - h
\end{aligned} \tag{A.7}$$

Operator Q_{LR}^S

$$E_{LR}^S = -8/3 d_1 - 4/3 e - 4/3 f$$

Constant	$r = 1$	$r = 0.75$	$r = 0.50$	$r = 0.25$	$r = 0$
J_1	-4.85	-4.93	-5.18	-6.08	-8.24
J_2	-0.16	-0.21	-0.28	-0.25	0.00
J_3	-0.11	-0.09	-0.06	-0.01	0.00
δ_L	0.20	0.15	0.09	0.02	0.00
δ_R	-1.23	-0.58	-0.17	-0.01	0.00

Table A.1: Numerical values of the new integrals for various values of the Wilson parameter r .

$$\begin{aligned}
E_{LR}^{SI} &= 8/3(l+m) - 8/3n - 4/3f^I \\
Et_{LR}^S &= J_1 + 2d_1 + c \\
Et_{LR}^{SI} &= J_2 + 2n \\
Et_{LR}^{SII} &= J_3 \\
Et_{RR} &= -w \\
Et_{RR}^I &= -w^I + 1/2(l+m) - 1/4s \\
Et_{RR}^{II} &= -3/4\delta_R \\
E_U &= -4/3d_2 \\
E_U^I &= 4/3(2d^I + q - h) \\
Et_U &= -d_2 \\
Et_U^I &= 2d^I + q - h
\end{aligned} \tag{A.8}$$

where the expressions and values for the constants d_1 , d_2 , f , v , w , c and e which determine the matching in the Wilson case, can be found in ref.[21]. The Clover constants l , m , n , q , h , s , d^I , f^I , v^I and w^I are defined in ref.[12] whereas the analytical expressions of δ_L and δ_R are given in ref.[13]. We have found small numerical discrepancies between our estimates for d^I , f^I , h and v^I and the values quoted in ref.[12]. Our results for $r = 1.0$ are $d^I = -4.13$, $f^I = -3.64$, $h = -9.97$ and $v^I = -6.72$ to be compared to $d^I = -4.04$, $f^I = -3.63$, $h = -9.88$ and $v^I = -6.69$ from Table 3 of ref.[12]. We have used the former to obtain all our results which agree with those recently and independently obtained in ref.[29].

The only new constants are J_1 , J_2 and J_3 defined as

$$\begin{aligned}
J_1 &= \frac{1}{\pi^2} \int_{-\pi}^{\pi} d^4k \left[\frac{\theta(1-k^2)}{k^4} - \frac{\Delta_4}{4\Delta_1\Delta_2^2} + \frac{\Delta_5}{4\Delta_1\Delta_2^2} - \frac{r^4\Delta_1^2}{\Delta_2^2} - \frac{r^2\Delta_4}{2\Delta_2^2} \right] \\
J_2 &= \frac{1}{\pi^2} \int_{-\pi}^{\pi} d^4k \left[\frac{r^2\Delta_4^2}{8\Delta_1\Delta_2^2} - \frac{r^2(\Delta_4 - \Delta_5)}{2\Delta_2^2} \right]
\end{aligned}$$

$$J_3 = \frac{1}{\pi^2} \int_{-\pi}^{\pi} d^4k \left[\frac{r^4 \Delta_4^2}{16 \Delta_2^2} - \frac{r^4 \Delta_1 (\Delta_4 - \Delta_5)}{4 \Delta_2^2} \right] \quad (\text{A.9})$$

where

$$\begin{aligned} \Delta_1 &= \sum_{\mu} \sin^2 \frac{q_{\mu}}{2} \\ \Delta_2 &= \sum_{\mu} \sin^2 q_{\mu} + 4 r^2 \Delta_1^2 \\ \Delta_4 &= \sum_{\mu} \sin^2 q_{\mu} \\ \Delta_5 &= \sum_{\mu} \sin^2 q_{\mu} \sin^2 \frac{q_{\mu}}{2} \end{aligned} \quad (\text{A.10})$$

In Table A.1, we give the numerical values of J_i , $i = 1, 2, 3$ for several values of the Wilson parameter r . We also give the constants δ_L and δ_R because in ref.[13] they are not presented explicitly.

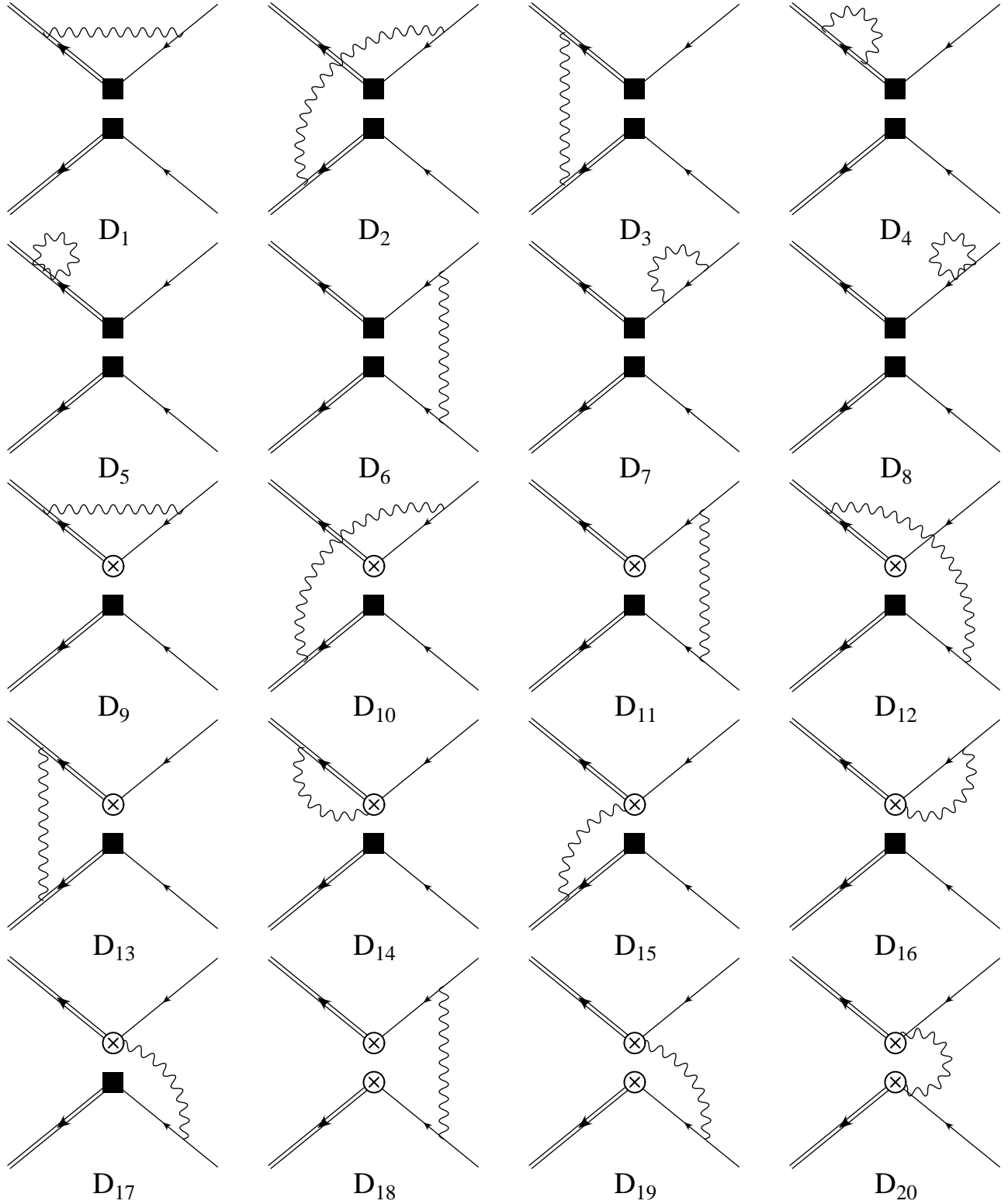


Figure 1: *Feynman Diagrams for the continuum-lattice matching. Up-down replicas and t -channel diagrams are not shown. For the $\Delta B = 0$ operators only s -channel diagrams contribute, penguin diagrams are not considered and the arrows in the lower fermionic lines must be inverted.*

References

- [1] F. Gabbiani *et al.*, Nucl. Phys. **B477** (1996) 321.
- [2] M. Beneke *et al.*, Phys. Rev. **D54** (1996) 4419.
- [3] V. L. Chernyak, Nucl. Phys. **B457** (1995) 96;
M. Neubert and C. T. Sachrajda, Nucl. Phys. **B483** (1997) 339.
- [4] G. Martinelli *et al.*, Nucl. Phys. **B445** (1995) 81.
- [5] V. Gimenez *et al.*, *Non-perturbative renormalization of the lattice heavy-light axial current in the static limit*, unpublished.
- [6] M. Crisafulli *et al.*, Nucl. Phys. **B457** (1995) 594;
V. Gimenez *et al.*, Phys. Lett. **B393** (1997) 124.
- [7] E. Eichten, in *Field Theory on the Lattice*, Nucl. Phys. **B**(Proc. Suppl)**4** (1988) 170.
- [8] P. Pascual and R. Tarrach, *QCD: Renormalization for the practitioner*, Springer Verlag 1984, ISBN: 3 540 12908 1.
- [9] K. G. Wilson, Phys. Rev. **D10** (1974) 2445.
- [10] B. Sheikholeslami and R. Wohlert, Nucl. Phys. **B259** (1985) 572.
- [11] G. Heatlie *et al.*, Nucl. Phys. **B352** (1991) 226; Nucl. Phys. **B**(Proc. Suppl)**17** (1990) 607;
E. Gabrielli *et al.*, Nucl. Phys. **B**(Proc. Suppl)**20** (1991) 448.
- [12] A. Borrelli and C. Pittori, Nucl. Phys. **B385** (1992) 502.
- [13] A. Borrelli *et al.*, Nucl. Phys. **B409** (1993) 382.
- [14] A. J. Buras and P. H. Weisz, Nucl. Phys. **B333** (1990) 66;
M. J. Dugan and B. Grinstein, Phys. Lett. **B256** (1991) 239;
M. Ciuchini *et al.*, Nucl. Phys. **B523** (1998) 501.
- [15] W. Siegel, Phys. Lett. **B84** (1979) 193.
- [16] G. Altarelli *et al.*, Nucl. Phys. **B187** (1981) 461.
- [17] G. 't Hooft and M. Veltman, Nucl. Phys. **B44** (1972) 189;
D.A. Akyeampong and R. Delbourgo, Nuovo Cim. **A17** (1973) 578, **A18** (1973) 94, **A19** (1974) 219.
- [18] G. Parisi, in "High Energy Physics - 1980", Proceedings of the XXth International Conference, Madison, Wisconsin, eds. L. Durand and L.G. Pondrom (American Institute of Physics, New York, 1981).
- [19] G.P. Lepage and P.B. Mackenzie, Nucl. Phys. B (Proc. Suppl.) **20** (1992) 173;
Phys. Rev. **D48** (1993) 2250.
- [20] M. Crisafulli *et al.*, hep-lat 9707025.

- [21] J. M. Flynn *et al*, Phys. Rev. **D43** (1991) 3709.
- [22] V. Gimenez and G. Martinelli, Phys. Lett. **B398** (1997) 135.
- [23] H. Wittig, Int. J. Mod. Phys. **A12** (1997) 4477.
- [24] C. Bernard, Nucl. Phys. B (Proc. Suppl.) **34** (1994) 47.
- [25] O. F. Hernández and B. R. Hill, Phys. Rev. **D50** (1994) 495.
- [26] V. Gimenez, Nucl. Phys. **B401** (1993) 116;
M. Ciuchini *et al*, Phys. Lett. **B388** (1996) 167;
G. Buchalla, Phys. Lett. **B395** (1997) 364.
- [27] V. Gimenez, Nucl. Phys. Proc. Suppl. **63** (1998) 371.
- [28] UKQCD Collaboration, A. K. Ewing *et al*, Phys. Rev. **D54** (1996) 3526.
- [29] M. di Pierro and C. T. Sachrajda, Nucl. Phys. **B534** (1998) 373.